A Posteriori Finite Element Output Bounds for the Incompressible Navier–Stokes Equations; Application to a Natural Convection Problem*

L. Machiels[†], J. Peraire[‡], and A. T. Patera[†]

April 27, 1999

Abstract

We present a new Neumann-subproblem *a posteriori* finite element procedure for the efficient calculation of rigorous, constant–free, sharp lower and upper bounds for linear and nonlinear functional outputs of the incompressible Navier-Stokes equations. We formulate the bound procedure; derive and discuss a bound error expression; and demonstrate the capabilities of the method with numerical results obtained for natural convection problems. We also implement an optimal adaptive refinement strategy based on a local elemental decomposition of the bound gap.

1 Introduction and Motivation

In typical design problems, engineers are rarely interested in the entire field solution; only some selected characteristic metrics — or outputs — of the system are relevant. As an example, we consider the problem of cooling electronic components by natural convection of air in the enclosure represented in Fig. 1(a), where the temperature θ is fixed on boundary Γ_0, a heat flux q is imposed on segments Γ_1, Γ_2, and Γ_3, and $\partial\Omega \setminus \cup_{i=0}^{3} \Gamma_i$ is insulated. The fluid flow and the temperature field are described by a system of partial differential equations; in our example, the Boussinesq approximation applies, and

*MIT FML Report 99-4. Submitted to Journal of Computational Physics. Address all correspondence to Dr L. Machiels c/o Prof. A. T. Patera, Room 3-264, M.I.T., 77 Massachusetts Avenue, Cambridge, MA, 02139, USA, machiels@mit.edu.

†Department of Mechanical Engineering, Massachusetts Institute of Technology.

‡Department of Aeronautics and Astronautics, Massachusetts Institute of Technology.

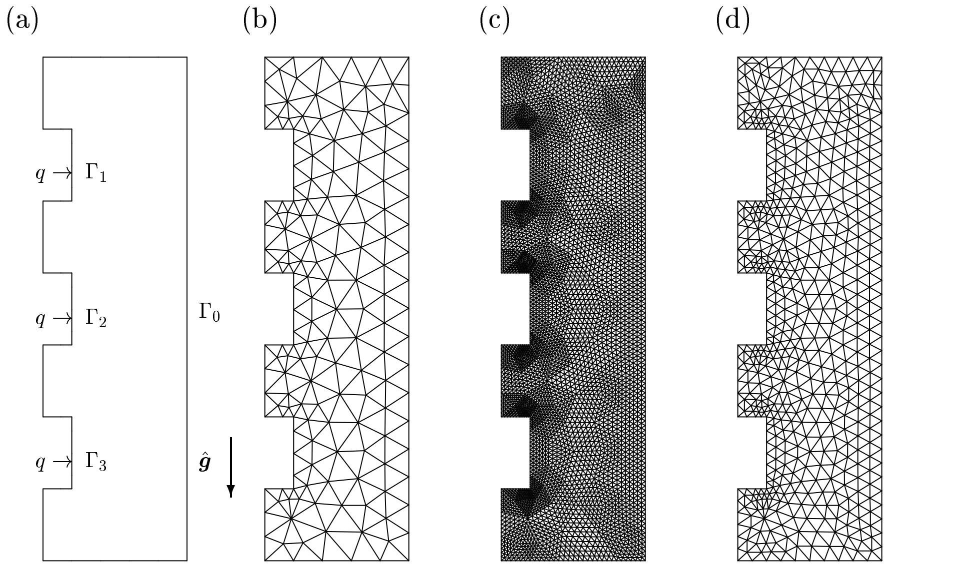

Figure 1: (a): Domain Ω. (b): "Optimistic" coarse mesh, $\mathcal{T}_H$. (c): "Conservative" fine mesh, $\mathcal{T}_h = \mathcal{T}_{H/6}$. (d): Coarse mesh $\mathcal{T}_{H/2}$.

the flow field is thus described by the incompressible Navier-Stokes equations coupled to a temperature equation. Given an input heat flux q, we wish to determine whether the mean temperature over Γ_1, $s = \frac{1}{\Gamma_1}\int_{\Gamma_1} \theta\, ds$, is within an acceptable design interval, $\mathcal{I}_{\mathrm{des}} = [s_{\mathrm{lo}}, s_{\mathrm{up}}]$; in practice, many different fluxes q must be tested, so there is a premium on efficiency. Much more complex design questions can also be addressed.

In a classical simulation design approach, the output of interest is evaluated from an approximate solution of the original problem. In the problem of cooling electronic components, Fig. 1(a), we first evaluate the output of interest $s_\delta = S(\boldsymbol{u}_\delta, p_\delta, \theta_\delta)$ from an approximate field solution $(\boldsymbol{u}_\delta, p_\delta, \theta_\delta)$ — here $\boldsymbol{u}_\delta$ is the velocity field, p_δ is the pressure field, θ_δ is the temperature field, and δ denotes the diameter of the discretization mesh $\mathcal{T}_\delta$. One then verifies whether $s_\delta \in \mathcal{I}_{\mathrm{des}}$, and the heat flux q is accepted or rejected accordingly. The shortcoming of the classical approach resides in the choice of the discretization mesh $\mathcal{T}_\delta$. If one chooses an "optimistic" relatively coarse mesh $\mathcal{T}_H$, Fig. 1(b), the calculation is *inexpensive* but also *uncertain* since neither $s_H \in \mathcal{I}_{\mathrm{des}}$ implies $s \in \mathcal{I}_{\mathrm{des}}$, nor $s_H \notin \mathcal{I}_{\mathrm{des}}$ implies $s \notin \mathcal{I}_{\mathrm{des}}$. If, instead, one chooses a "conservative" sufficiently fine mesh $\mathcal{T}_h$, Fig. 1(c) — the mesh $\mathcal{T}_h$ represented on the Figure is obtained by dividing each triangle of mesh $\mathcal{T}_H$ into 36 self-similar triangles — then $s_h \approx s$ with reasonable *certainty*, but

s_h is now very *expensive* to compute.

This paper presents a new approach which offers great promise in reconciling these conflicting requirements. We propose to construct a pair of output bound approximations, the estimators s_H^+ and s_H^-, computed predominantly on the mesh $\mathcal{T}_H$ and with the following attributes.

A1 As $H \to h$, we have $s_H^+ \to s_h$ from above and $s_H^- \to s_h$ from below $\forall H \leq H^*$. Here H^* is an unknown threshold discretization parameter; a detailed discussion of H^* will be given subsequently.

A2 If we define the half bound gap $\Delta_H = \frac{1}{2}(s_H^+ - s_H^-)$, we have $\Delta_H \leq \eta |s_H - s_h|$ as $H \to h$, with η independent of H. This property guarantees the optimal convergence rate and sharpness of the bounds, provided the effectivity factor η is not too large.

A3 The bound gap Δ_H admits elemental decomposition $\Delta_H = \sum_{T_H \in \mathcal{T}_H} \Delta_{T_H}$, with $\Delta_{T_H} \geq 0$, for all elements T_H in $\mathcal{T}_H$; this will serve for adaptive refinement.

A4 The work required to evaluate s_H^+ and s_H^- is substantially smaller that the work necessary for the computation s_h, provided $H \ll h$.

Note that attribute A2 is important not only for efficiency, but also to ensure the "well-posedness" of the estimator formulation when $H^* < \infty$.

In our example, Fig. 1(a), the bound-based design would proceed as follows. Given a heat flux q, we choose an initial mesh $\mathcal{T}_H$, and we compute s_H^+ and s_H^-. Next, we define $\mathcal{I}_{\mathrm{b}} = [s_H^-, s_H^+]$; according to attribute A1 (provided $H \leq H^*$), if $\mathcal{I}_{\mathrm{b}} \in \mathcal{I}_{\mathrm{des}}$, we can accept q; if $\mathcal{I}_{\mathrm{b}} \in \mathbb{R} \setminus \mathcal{I}_{\mathrm{des}}$, we can reject q; otherwise, we use property A2, that is, we narrow the bound gap by taking a finer mesh (a smaller H), and we repeat the procedure. In the latter case, attribute A3 is important as it allows us to optimally refine the mesh through an adaptive procedure. Attribute A4 ensures that the complete procedure is much less expensive than directly computing s_h.

We illustrate these concepts by fixing a design interval, say $\mathcal{I}_{\mathrm{des}} = [0.26, 0.28]$; for a typical choice of the flux q and of the parameters governing the problem, the outcome of the bound procedure performed on the coarse mesh $\mathcal{T}_H$ (Fig. 1(b)) is $s_h = 0.274 \pm 7.8\%$, or $s_h \in \mathcal{I}_{\mathrm{b}} = [0.253, 0.296]$. According to our specification of $\mathcal{I}_{\mathrm{des}}$, one can not decide whether to accept or reject the heat flux q. Thus, we refine the mesh. The mesh $\mathcal{T}_{H/2}$ is obtained by dividing each triangle of mesh $\mathcal{T}_H$ into four triangles (dividing each edge into two edges); see Fig. 1(d). For this new mesh the bound procedure yields $s_h = 0.276 \pm 1.3\%$, or $s_h \in \mathcal{I}_{\mathrm{b}} = [0.272, 0.279]$. Since now

$\mathcal{I}_{\rm b} \in \mathcal{I}_{\rm des}$, we can safely accept the flux q. Note that, in this example, we have not used attribute A3 which allows optimal adaptive refinement. Examples with adaptivity will be given in Section 4.

The procedure is an extension of our recent general error control strategy [14, 15, 17, 11, 8], and may be viewed as an implicit Aubin-Nitsche construction; for a review, see [9]. In particular, in [13], an early application of the technique to the Stokes equations is presented. Our method is indebted to, but considerably generalizes, earlier finite element *a posteriori* error estimation techniques in that we obtain quantitative constant-free bound — contrary to earlier explicit techniques [4] — for the output of interest — contrary to earlier implicit techniques [7, 3, 2]. Some aspects of the method are also analogous to certain domain decomposition techniques [12, 6].

The purpose of the present paper is (i) to give a detailed and complete account of the bound algorithm, (ii) to derive and discuss a bound error expression, and (iii) to demonstrate the attributes of the procedure with numerical examples. A complete and rigorous numerical analysis of the method is relegated to a future paper.

The paper is organized as follows. Section 2 contains the formulation of the bound procedure. We start by formulating the finite element discretization of the natural convection problem; we next introduce some preliminary definitions; and we then detail the bound algorithm. Finally, we derive a bound error expression. In Section 3, we present numerical results for two natural convection problems; we also implement an optimal adaptive refinement strategy based on the bound procedure. We conclude, in Section 4, by a review of the various attributes of the method. For the convenience of presentation, some mathematical developments have been collected in appendices.

2 Bound Procedure

This Section is divided into four parts. We first introduce the equations governing the natural convection problem considered, and we formulate the finite element approximation; in particular, to ease the subsequent discussion, we recall or introduce the necessary function spaces, finite element spaces, and forms. In the second part, we complete our definitions by introducing the ingredients particular to the bound method, namely the "broken" finite element spaces — which are characterized by relaxation of the continuity constraint of the finite element functions across edges of the coarse mesh — and the Taylor expansion and splitting of the nonlinear forms introduced in the first part. In the third part, after the introduction of the appropriate concepts and definitions, we detail and discuss the five steps of the bound construction. Finally, in the last part, we discuss the bounds error expression.

2.1 Problem statement

Given a two dimensional domain $\Omega \in \mathbb{R}^2$, we consider a problem of natural convection which is, in the Boussinesq approximation, described by

$$-\frac{\partial}{\partial x_j}\left(\frac{\partial u_i}{\partial x_j}+\frac{\partial u_j}{\partial x_i}\right)+\frac{\partial (u_j u_i)}{\partial x_j}+\frac{\partial p}{\partial x_i}=-\beta\theta\hat{g}_i \quad \text{in } \Omega, \tag{1}$$

$$\frac{\partial u_i}{\partial x_i}=0 \quad \text{in } \Omega, \tag{2}$$

$$-\frac{1}{\alpha}\frac{\partial^2 \theta}{\partial x_j \partial x_j}+\frac{\partial (u_j \theta)}{\partial x_j}=0 \quad \text{in } \Omega, \tag{3}$$

where the summation convention of repeated indices applies, $\boldsymbol{u}=(u_1,u_2)$ is the velocity field, p is the pressure field, θ is the temperature field, and $\hat{\boldsymbol{g}}=(\hat{g}_1,\hat{g}_2)$ is the unit vector indicating the direction of gravity. The flow is governed by two nondimensional parameters: the Prandtl number, α, and the Grashof number, β. We supplement Eqs. (1), (2), and (3) with the following boundary conditions,

$$\boldsymbol{u}|_{\partial\Omega}=0 \quad \text{and} \quad \begin{cases} \theta = 0 & \text{on } \Gamma_0, \\ \frac{1}{\alpha}\frac{\partial \theta}{\partial n}=g_N & \text{on } \Gamma_k, \text{ for } k=1,2,\cdots,K \\ \frac{\partial\theta}{\partial n}=0 & \text{on } \partial\Omega \setminus \cup_{k=0,1,\cdots,K}\Gamma_k, \end{cases} \tag{4}$$

where $\Gamma_k \subset \partial\Omega$, $\Gamma_k \cap \Gamma_l = \emptyset$ when $k \neq l$, and g_N is a heat flux.

2.1.1 Variational Formulation

Our point of departure for a finite element approximation of Eqs. (1), (2), and (3) is a variational formulation. We first recall the definitions of some function spaces and their associated norms and semi-norms. For $1 \leq p \leq +\infty$, we define the space

$$L^p(\Omega)=\{v:\Omega\rightarrow\mathbb{R}\,|\,v \text{ is measurable and}, \int_\Omega |v|^p\, d\Omega < +\infty\},$$

and its associated norm

$$||v||_{L^p(\Omega)}=(\int_\Omega |v|^p\, d\Omega)^{1/p}.$$

We also define

$$L^\infty(\Omega) = \{v : \Omega \to \mathbb{R} \,|\, \text{ess sup}\{|v(\boldsymbol{x})| \,|\, \boldsymbol{x} \in \Omega\} < +\infty\},$$

and the norm $||v||_\infty = \text{ess sup}\{|v(\boldsymbol{x})| \,|\, \boldsymbol{x} \in \Omega\}$. Let $\boldsymbol{\alpha} = (\alpha_1, \alpha_2)$ with α_1 and α_2 non-negative integers; then we define

$$D^{\boldsymbol{\alpha}} v = \frac{\partial^{|\boldsymbol{\alpha}|} v}{\partial x_1^{\alpha_1} \partial x_2^{\alpha_2}},$$

where $|\boldsymbol{\alpha}| = \alpha_1 + \alpha_2$. The Sobolev space $H^k(\Omega)$ (see, *e.g.*, [1]), k being a non-negative integer, is the space

$$H^k(\Omega) = \{v \in L^2(\Omega) \,|\, D^{\boldsymbol{\alpha}} v \in L^2(\Omega), \forall |\boldsymbol{\alpha}| \leq k\}.$$

We will also use the spaces

$$H_0^k(\Omega) = \{v \in H^k(\Omega) \,|\, v|_{\partial\Omega} = 0\}.$$

We finally introduce the norms and semi-norms associated with the spaces $H^k(\Omega)$,

$$||v||_{H^k(\Omega)} = \left(\sum_{|\boldsymbol{\alpha}| \leq k} \int_\Omega |D^{\boldsymbol{\alpha}} v|^2 \, d\Omega \right)^{1/2}, \quad |v|_{H^k(\Omega)} = \left(\sum_{|\boldsymbol{\alpha}| = k} \int_\Omega |D^{\boldsymbol{\alpha}} v|^2 \, d\Omega \right)^{1/2}.$$

We define now the function spaces $X = H_0^1(\Omega) \times H_0^1(\Omega)$, $M = L^2(\Omega)$,

$$X^\theta = \{v \in H^1(\Omega) \,|\, v|_{\Gamma_0} = 0\},$$

and $Y = X \times M \times X^\theta$. To facilitate the variational formulation of the problem, we define the following bilinear and trilinear forms

$$a : X \times X \to \mathbb{R}, \quad a(\boldsymbol{v}, \boldsymbol{w}) = \int_\Omega \left(\frac{\partial v_i}{\partial x_j} + \frac{\partial v_j}{\partial x_i} \right) \frac{\partial w_i}{\partial x_j} \, d\Omega,$$

$$a^\theta : X^\theta \times X^\theta \to \mathbb{R}, \quad a^\theta(\phi, \rho) = \frac{1}{\alpha} \int_\Omega \frac{\partial \phi}{\partial x_i} \frac{\partial \rho}{\partial x_i} \, d\Omega,$$

$$b : X \times M \to \mathbb{R}, \quad b(\boldsymbol{v}, r) = -\int_\Omega \frac{\partial v_i}{\partial x_i} r \, d\Omega,$$

$$c : X \times X \times X \to \mathbb{R}, \quad c(\boldsymbol{v}_1, \boldsymbol{v}_2, \boldsymbol{w}) = -\int_\Omega (v_{1i} v_{2j}) \frac{\partial w_i}{\partial x_j} \, d\Omega,$$

$$c^\theta : X^\theta \times X \times X^\theta \to \mathbb{R}, \quad c^\theta(\phi, \boldsymbol{v}, \rho) = -\int_\Omega (\phi v_j) \frac{\partial \rho}{\partial x_j} \, d\Omega,$$

$$d : X^\theta \times X \to \mathbb{R}, \quad d(\phi, \boldsymbol{w}) = \beta \int_\Omega \phi w_i \hat{g}_i \, d\Omega.$$

Finally, we introduce the "natural convection form",

$$\mathcal{A}((\boldsymbol{v},q,\phi),(\boldsymbol{w},r,\rho)) = a(\boldsymbol{v},\boldsymbol{w}) + a^\theta(\phi,\rho) + b(\boldsymbol{v},r) + b(\boldsymbol{w},q) \\ + c(\boldsymbol{v},\boldsymbol{v},\boldsymbol{w}) + c^\theta(\phi,\boldsymbol{v},\rho) + d(\phi,\boldsymbol{w}) - \langle g_N,\rho\rangle_N\,, \quad (5)$$

where

$$\langle g_N,\rho\rangle_N = \sum_{0<k\leq K} \int_{\Gamma_k} g_N\rho|_{\Gamma_k}\, d\Gamma,$$

(we assume $g_N \in L^2(\cup_{k=1,\cdots,K}\Gamma_k)$). The variational formulation of Eqs. (1), (2), and (3), with boundary conditions (4), then consists in finding $(\boldsymbol{u},p,\theta) \in Y$ such that

$$\mathcal{A}((\boldsymbol{u},p,\theta),(\boldsymbol{v},q,\phi)) = 0, \quad \forall (\boldsymbol{v},q,\phi) \in Y. \quad (6)$$

As indicated in the Introduction, we suppose that we are not directly interested in the complete field solution $(\boldsymbol{u},p,\theta)$, but that we wish to evaluate an output of interest $s = S(\boldsymbol{u},p,\theta)$; we assume that the form S can be expressed as

$$S(\boldsymbol{v},q,\phi) = c_0 + \ell(\boldsymbol{v},q,\phi) + m(\boldsymbol{v},\boldsymbol{v}), \quad (7)$$

where $c_0 \in \mathbb{R}$, $\ell : Y \to \mathbb{R}$ is a bounded linear functional, and $m : X \times X \to \mathbb{R}$ is a countinous bilinear functional such that

$$m(\boldsymbol{v},\boldsymbol{v}) \leq C||\boldsymbol{v}||^2_{L^2(\Omega)}, \quad (8)$$

with $C > 0$; he norm in the product space $L^2(\Omega) \times L^2(\Omega)$ is defined by $||\boldsymbol{v}||^2_{L^2(\Omega)} = ||v_1||^2_{L^2(\Omega)} + ||v_2||^2_{L^2(\Omega)}$. In addition, since in this formulation the pressure p is defined only to within a constant, we require that

$$\ell(\boldsymbol{0},1,0) = 0. \quad (9)$$

2.1.2 Finite Element Formulation

We will now define a finite element approximation of (6). We consider a (regular, uniform) triangulation $\mathcal{T}_\delta$ of the domain Ω, that is $\mathcal{T}_\delta$ is a set of triangles, T_δ, such that

$$\overline{\Omega} = \cup_{T_\delta \in \mathcal{T}_\delta} \overline{T_\delta} \quad \text{and} \quad T_\delta \cap T'_\delta = \emptyset \quad \text{if} \quad T_\delta \neq T'_\delta,$$

where $\overline{A}$ denotes the closure of $A \subset \mathbb{R}^2$, and δ is the diameter of the triangulation $\mathcal{T}_\delta$,

$$\delta = \max_{T_\delta \in \mathcal{T}_\delta} \operatorname{diam}(T_\delta), \quad \text{where} \quad \operatorname{diam}(T_\delta) = \max_{\boldsymbol{x},\boldsymbol{y} \in T_\delta} |\boldsymbol{x} - \boldsymbol{y}|.$$

For a given triangulation $\mathcal{T}_\delta$, we will denote by $\mathcal{T}_{\delta/2}, \mathcal{T}_{\delta/3}, \cdots$ the refinements of $\mathcal{T}_\delta$ obtained by dividing each triangle of T_δ into $2^2, 3^2, ...$ self-similar triangles. In particular, we will say that $\mathcal{T}_{\delta'}$ is a refinement of $\mathcal{T}_\delta$ if there is an integer $n > 0$ such that $\mathcal{T}_{\delta'} = \mathcal{T}_{\delta/n}$.

In this work, we choose the Crouzeix-Raviart finite element spaces for the velocity and the pressure [5], that is, the approximate velocity $\boldsymbol{u}_\delta \in X_\delta$ and the approximate pressure $p_\delta \in M_\delta$, where

$$\begin{aligned} X_\delta &= \{\boldsymbol{v} \in H_0^1(\Omega) \times H_0^1(\Omega) \,|\, v_i|_{T_\delta} \in \mathbb{P}_2(T_\delta) \oplus B_3(T_\delta), \forall T_\delta \in \mathcal{T}_\delta\}, \\ M_\delta &= \{p \in L^2(\Omega) \,|\, p|_{T_\delta} \in \mathbb{P}_1(T_\delta), \forall T_\delta \in \mathcal{T}_\delta\}. \end{aligned}$$

Here $\mathbb{P}_p(T_\delta)$ is the space of all polynomials of degree $\leq p$ defined on T_δ, and $B_3(T_\delta)$ denotes the space of bubble functions of degree 3 on T_δ. We also use the standard quadratic elements for the temperature field, $\theta_\delta \in X_\delta^\theta$, where

$$X_\delta^\theta = \{\phi \in H^1(\Omega) \,|\, \phi|_{T_\delta} \in \mathbb{P}_2(T_\delta), \forall T_\delta \in \mathcal{T}_\delta, \text{ and } \phi|_{\Gamma_0} = 0\}.$$

Finally, we define the solution space as the product space $Y_\delta = X_\delta \times M_\delta \times X_\delta^\theta$.

The finite element method for Eqs. (1), (2), and (3) with the boundary conditions (4) consists in the construction of an approximate solution $(\boldsymbol{u}_\delta, p_\delta, \theta_\delta) \in Y_\delta$ is such that

$$\mathcal{A}((\boldsymbol{u}_\delta, p_\delta, \theta_\delta), (\boldsymbol{v}, q, \phi)) = 0, \quad \forall (\boldsymbol{v}, q, \phi) \in Y_\delta.$$

We now assume that we are given two triangulations: $\mathcal{T}_H$, the coarse mesh, and $\mathcal{T}_h$, the fine mesh, with $\mathcal{T}_h$ a refinement of $\mathcal{T}_H$, and $h \ll H$. Therefore, we have $Y_H \subset Y_h$, where Y_H is the finite element space associated with the triangulation $\mathcal{T}_H$, and Y_h is the finite element space associated with $\mathcal{T}_h$. The associated coarse-space and fine-space approximations, $(\boldsymbol{u}_H, p_H, \phi_H)$ and $(\boldsymbol{u}_h, p_h, \phi_h)$, exhibit complementary advantages and disadvantages. The fine space solution, $(\boldsymbol{u}_h, p_h, \phi_h) \in Y_h$, which satisfies the discrete equations

$$\mathcal{A}((\boldsymbol{u}_h, p_h, \theta_h), (\boldsymbol{v}, q, \phi)) = 0, \quad \forall (\boldsymbol{v}, q, \phi) \in Y_h, \tag{10}$$

yields a very good approximation, $s_h = S(\boldsymbol{u}_h, p_h, \theta_h)$, to the exact output s; nevertheless, the computational effort required to obtain $(\boldsymbol{u}_h, p_h, \theta_h)$ will typically be prohibitive. In contrast, the coarse-space solution $(\boldsymbol{u}_H, p_H, \theta_H) \in Y_H$, which satisfies the discrete equations

$$\mathcal{A}((\boldsymbol{u}_H, p_H, \theta_H), (\boldsymbol{v}, q, \phi)) = 0, \quad \forall (\boldsymbol{v}, q, \phi) \in Y_H,$$

can be obtained with relatively modest computational effort; nevertheless the fidelity of the corresponding approximate output, $s_H = S(\boldsymbol{u}_H, p_H, \theta_H)$, is no longer assured.

2.2 Preliminaries

The formulation of the bound algorithm requires the definition of particular finite element spaces, the "broken" spaces, which are obtained as extensions of the classical finite element spaces by relaxing the continuity of the finite element basis functions across edges of the coarse mesh. Moreover, due to the nonlinearity, noncoercivity, and nonsymmetry of the problem, we must also expand the nonlinear forms $\mathcal{A}$ and S into other linear, bilinear, and trilinear forms; we then further decompose some of these new forms into coercive — with respect to divergence-free functions — and noncoercive parts, and symmetric and antisymmetric components.

2.2.1 "Broken" spaces

We denote by $\Gamma(\mathcal{T}_H)$ the set of edges γ of $\mathcal{T}_H$. We define the "broken" finite element spaces as

$$\begin{aligned}
\hat{X}_H =& \{\boldsymbol{v} \in L^2(\Omega) \times L^2(\Omega) \,|\, v_i|_{T_H} \in \mathbb{P}_2(T_H) \oplus B_3(T_H), \forall T_H \in \mathcal{T}_H\},\\
\hat{X}_h =& \{\boldsymbol{v} \in L^2(\Omega) \times L^2(\Omega) \,|\, v_i|_{T_H} \in H^1(T_H) \times H^1(T_H), \forall T_H \in \mathcal{T}_H;\\
& v_i|_{T_h} \in \mathbb{P}_2(T_h) \oplus B_3(T_h), \forall T_h \in \mathcal{T}_h\},\\
\hat{X}_H^{\theta} =& \{\phi \in L^2(\Omega) \,|\, \phi|_{T_H} \in \mathbb{P}_2(T_H), \forall T_H \in \mathcal{T}_H\}.\\
\hat{X}_h^{\theta} =& \{\phi \in L^2(\Omega) \,|\, \phi|_{T_H} \in H^1(T_H), \forall T_H \in \mathcal{T}_H; \phi|_{T_h} \in \mathbb{P}_2(T_h), \forall T_h \in \mathcal{T}_h\}.
\end{aligned}$$

If $\hat{Y}_H = \hat{X}_H \times M_H \times \hat{X}_H^{\theta}$ and $\hat{Y}_h = \hat{X}_h \times M_h \times \hat{X}_h^{\theta}$, we have $Y_H \subset \hat{Y}_H$ and $Y_h \subset \hat{Y}_h$.

We also define the "hybrid flux" spaces

$$\begin{aligned}
Q_H &= \{\boldsymbol{z} \in L^2(\Gamma(\mathcal{T}_H)) \times L^2(\Gamma(\mathcal{T}_H)) \,|\, z_i|_{\gamma} \in \mathbb{P}_4(\gamma), \forall \gamma \in \Gamma(\mathcal{T}_H)\},\\
Q_H^{\theta} &= \{z \in L^2(\Gamma(\mathcal{T}_H)) \,|\, z|_{\gamma} \in \mathbb{P}_4(\gamma), \forall \gamma \in \Gamma(\mathcal{T}_H); z|_{\gamma} = 0, \forall \gamma \in \partial\Omega \setminus \Gamma_0\}.
\end{aligned}$$

The reason for using quartic polynomials ($\mathbb{P}_4$) will become apparent in the bound procedure. (In fact $\mathbb{P}_2$ polynomials would be sufficient.) We define the product spaces $Z_H = Q_H \times Q_H^\theta$, and the form $B : (X_h \times M_h) \times Z_H \to \mathbb{R}$,

$$B((\boldsymbol{v},\theta);(\boldsymbol{z},z^\theta)) = \sum_{\gamma\in\Gamma(\mathcal{T}_H)} \int_\gamma ([v_i]_\gamma z_i|_\gamma + [\theta]_\gamma z^\theta|_\gamma)\,d\gamma,$$

where $[v]_\gamma$ denotes the jump in v across γ when $\gamma \in \Omega$ and the trace of v when $\gamma \in \partial\Omega$. Note that we have the following equivalence condition

$$Y_H = \{(\boldsymbol{v},q,\phi) \in \hat{Y}_H \,|\, B((\boldsymbol{v},\phi);(\boldsymbol{z},z^\theta)) = 0, \forall(\boldsymbol{z},z^\theta) \in Z_H\}.$$

2.2.2 Form Expansions

We define

$$\begin{aligned}\mathcal{E}((\bar{\boldsymbol{u}},\bar{p},\bar{\theta});(\boldsymbol{v},q,\phi),(\boldsymbol{w},r,\rho)) = \\ \mathcal{A}(\bar{\boldsymbol{u}}+\boldsymbol{v},\bar{p}+q,\bar{\theta}+\phi),(\boldsymbol{w},r,\rho)) - \mathcal{A}((\bar{\boldsymbol{u}},\bar{p},\bar{\theta}),(\boldsymbol{w},r,\rho)).\end{aligned} \quad (11)$$

Since $\mathcal{A}((\boldsymbol{v},q,\phi),(\boldsymbol{w},r,\rho))$ is quadratic in $(\boldsymbol{v},\phi)$, we can express $\mathcal{E}$ as

$$\begin{aligned}\mathcal{E}((\bar{\boldsymbol{u}},\bar{p},\bar{\theta});(\boldsymbol{v},q,\phi),(\boldsymbol{w},r,\rho)) = \\ E((\bar{\boldsymbol{u}},\bar{p},\bar{\theta});(\boldsymbol{v},q,\phi),(\boldsymbol{w},r,\rho)) + F((\boldsymbol{v},\phi),(\boldsymbol{v},\phi),(\boldsymbol{w},\rho)),\end{aligned} \quad (12)$$

where E is linear in $(\boldsymbol{v},q,\phi)$ and $(\boldsymbol{w},r,\rho)$, and F is trilinear. The form E represents the linearized natural convection form (5). More precisely we have

$$\begin{aligned}E((\bar{\boldsymbol{u}},\bar{p},\bar{\theta});(\boldsymbol{v},q,\phi),(\boldsymbol{w},r,\rho)) = \\ E_0((\boldsymbol{v},q,\phi),(\boldsymbol{w},r,\rho)) + E_1((\bar{\boldsymbol{u}},\bar{\theta});(\boldsymbol{v},\phi),(\boldsymbol{w},\rho)),\end{aligned}$$

where

$$E_0((\boldsymbol{v},q,\phi),(\boldsymbol{w},r,\rho)) = a(\boldsymbol{v},\boldsymbol{w}) + a^\theta(\phi,\rho) + b(\boldsymbol{v},r) + b(\boldsymbol{w},q), \quad (13)$$

and

$$\begin{aligned}E_1((\bar{\boldsymbol{u}},\bar{\theta});(\boldsymbol{v},\phi),(\boldsymbol{w},\rho)) = c(\bar{\boldsymbol{u}},\boldsymbol{v},\boldsymbol{w}) + c(\boldsymbol{v},\bar{\boldsymbol{u}},\boldsymbol{w}) + d(\phi,\boldsymbol{w}) \\ + c^\theta(\bar{\theta},\boldsymbol{v},\rho) + c^\theta(\phi,\bar{\boldsymbol{u}},\rho).\end{aligned}$$

The form F is expressed as,

$$F((\boldsymbol{v}_1, \phi_1), (\boldsymbol{v}_2, \phi_2), (\boldsymbol{w}, \rho)) = \\ \frac{1}{2}\left[c(\boldsymbol{v}_1, \boldsymbol{v}_2, \boldsymbol{w}) + c(\boldsymbol{v}_2, \boldsymbol{v}_1, \boldsymbol{w}) + c^\theta(\phi_1, \boldsymbol{v}_2, \rho) + c^\theta(\phi_2, \boldsymbol{v}_1, \rho)\right],$$

and is symmetric in $(\boldsymbol{v}_1, \phi_1)$ and $(\boldsymbol{v}_2, \phi_2)$. Note that, if we define the space of discretely divergence-free functions

$$V_h = \{\boldsymbol{v} \in X_h \mid b(\boldsymbol{v}, q) = 0, \forall q \in M_h\},$$

then E_0 is positive definite with respect to $V_h \times M_h \times X_h^\theta$, that is

$$E_0((\boldsymbol{v}, q, \phi), (\boldsymbol{v}, q, \phi)) = a(\boldsymbol{v}, \boldsymbol{v}) + a^\theta(\phi, \phi) > 0,$$

for all $\boldsymbol{v} \in V_h$, $q \in M_h$, and $\phi \in X_h^\theta$ with $(\boldsymbol{v}, \phi) \neq (\mathbf{0}, 0)$.

Now, we expand the output, Eq. (7), as

$$S(\bar{\boldsymbol{u}} + \boldsymbol{v}, \bar{p} + q, \bar{\theta} + \rho) - S(\bar{\boldsymbol{u}}, \bar{p}, \bar{\theta}) = L((\bar{\boldsymbol{u}}, \bar{p}, \bar{\theta}); (\boldsymbol{v}, q, \phi)) + M(\boldsymbol{v}, \boldsymbol{v}),$$

where

$$L((\bar{\boldsymbol{u}}, \bar{p}, \bar{\theta}); (\boldsymbol{v}, q, \phi)) = \ell(\boldsymbol{v}, q, \phi) + m(\bar{\boldsymbol{u}}, \boldsymbol{v}) + m(\boldsymbol{v}, \bar{\boldsymbol{u}}), \tag{14}$$

and $M(\boldsymbol{v}, \boldsymbol{v}) = m(\boldsymbol{v}, \boldsymbol{v})$.

Finally, we define the following primal and dual residuals

$$\mathcal{R}^{\mathrm{pr}}((\bar{\boldsymbol{u}}, \bar{p}, \bar{\theta}); (\boldsymbol{v}, q, \phi)) = -\mathcal{A}((\bar{\boldsymbol{u}}, \bar{p}, \bar{\theta}), (\boldsymbol{v}, q, \phi)), \tag{15}$$

and

$$\mathcal{R}^{\mathrm{du}}((\bar{\boldsymbol{u}}, \bar{p}, \bar{\theta}); (\boldsymbol{\psi}_0, \lambda_0, \mu_0); (\boldsymbol{\psi}_1, \mu_1); (\boldsymbol{v}, q, \phi)) = -L((\bar{\boldsymbol{u}}, \bar{p}, \bar{\theta}); (\boldsymbol{v}, q, \phi)) \\ - E_0((\boldsymbol{\psi}_0, \lambda_0, \mu_0), (\boldsymbol{v}, q, \phi)) - E_1((\bar{\boldsymbol{u}}, \bar{\theta}); (\boldsymbol{\psi}_1, \mu_1), (\boldsymbol{v}, \phi)). \tag{16}$$

Note that, if we define $\bar{\boldsymbol{e}} = \boldsymbol{u}_h - \bar{\boldsymbol{u}}$, $\bar{\varepsilon} = p_h - \bar{p}$, and $\bar{e}^\theta = \theta_h - \bar{\theta}$, then it follows, from Eqs. (10), (11), and (15), that

$$\mathcal{E}((\bar{\boldsymbol{u}}, \bar{p}, \bar{\theta}); (\bar{\boldsymbol{e}}, \bar{\varepsilon}, \bar{e}^\theta), (\boldsymbol{v}, q, \phi)) = \mathcal{R}^{\mathrm{pr}}((\bar{\boldsymbol{u}}, \bar{p}, \bar{\theta}); (\boldsymbol{v}, q, \phi)), \forall (\boldsymbol{v}, q, \phi) \in Y_h. \tag{17}$$

2.3 Algorithm

The bound algorithm proceeds in five steps, which we detail here. The computation is initiated by two global solves on the coarse mesh $\mathcal{T}_H$: one for the initial nonlinear (primal) problem, Step 1, and one for the adjoint linear (dual) problem, Step 2. In Step 3, we compute the hybrid fluxes which will serve as boundary conditions for the local Neumann subproblems Step 4 — after the elimination, by fine mesh projections, of the indefinite terms associated with the incompressibility constraint. Step 5 proceeds with the bounds calculation, using the "reconstructed errors" obtained as the solution of the local subproblems in Step 4.

2.3.1 Step 1

We first compute $(\boldsymbol{u}_H, p_H, \theta_H) \in Y_H$ as the solution of the *primal* problem

$$\mathcal{A}((\boldsymbol{u}_H, p_H, \theta_H); (\boldsymbol{v}, q, \phi)) = 0, \quad \forall(\boldsymbol{v}, q, \phi) \in Y_H.$$

In practice, we find $(\boldsymbol{u}_H, p_H, \theta_H) = (\boldsymbol{u}_H^k, p_H^k, \theta_H^k)$ using Newton iteration, which is conveniently expressed as:

1. Select an initial guess $(\boldsymbol{u}_H^0, p_H^0, \theta_H^0) \in Y_H$ and set $k = 0$.
2. Find $(\boldsymbol{v}_H, q_H, \phi_H) \in Y_H$ such that

   $$E((\boldsymbol{u}_H^k, p_H^k, \theta_H^k), (\boldsymbol{v}_H, q_H, \phi_H), (\boldsymbol{w}, r, \rho)) = \\ \mathcal{R}^{\mathrm{pr}}((\boldsymbol{u}_H^k, p_H^k, \theta_H^k); (\boldsymbol{w}, r, \rho)), \quad \forall(\boldsymbol{w}, r, \rho) \in Y_H.$$

   Recall that E is the linearized natural convection form. The solvability of the divergence-free constraint system is ensured by the homogeneous Dirichlet boundary condition.
3. Set $k = k + 1$ and $(\boldsymbol{u}_H^k, p_H^k, \theta_H^k) = (\boldsymbol{u}_H^{k-1}, p_H^{k-1}, \theta_H^{k-1}) + (\boldsymbol{v}_H, q_H, \phi_H)$; then stop or go to 1, according to an appropriate stopping criterion.

2.3.2 Step 2

We compute the adjoint $(\boldsymbol{\psi}_H, \lambda_H, \mu_H) \in Y_H$ as the solution of the following *dual* problem

$$E((\boldsymbol{u}_H, p_H, \theta_H); (\boldsymbol{v}, q, \phi), (\boldsymbol{\psi}_H, \lambda_H, \mu_H)) = \\ - L((\boldsymbol{u}_H, p_H, \theta_H), (\boldsymbol{v}, q, \phi)), \quad \forall(\boldsymbol{v}, q, \phi) \in Y_H. \quad (18)$$

Again, the solvability of the constraint system is ensured by the homogeneous Dirichlet boundary condition and the condition

$$L((\boldsymbol{u}_H, p_H, \theta_H); (\mathbf{0}, 1, 0)) = 0,$$

which follows from our definition of the output, Eq. (9), and from Eq. (14).

2.3.3 Step 3

We now compute the primal and dual hybrid fluxes, $(\boldsymbol{z}, z^\theta)^{\mathrm{pr}} \in Z_H$ and $(\boldsymbol{z}, z^\theta)^{\mathrm{du}} \in Z_H$, which satisfy the equations

$$B((\boldsymbol{v}, \phi), (\boldsymbol{z}, z^\theta)^{\mathrm{pr}}) = \mathcal{R}^{\mathrm{pr}}((\boldsymbol{u}_H, p_H, \theta_H); (\boldsymbol{v}, q, \phi)), \quad \forall (\boldsymbol{v}, q, \phi) \in \hat{Y}_H, \tag{19}$$

and

$$B((\boldsymbol{v}, \phi), (\boldsymbol{z}, z^\theta)^{\mathrm{du}}) = \mathcal{R}^{\mathrm{du}}((\boldsymbol{u}_H, p_H, \theta_H); (\boldsymbol{\psi}_H, \lambda_H, \mu_H); (\boldsymbol{\psi}_H, \mu_H); (\boldsymbol{v}, q, \phi)), \quad \forall (\boldsymbol{v}, q, \phi) \in \hat{Y}_H. \tag{20}$$

To find a suitable solution of Eq. (19), we first form the approximation, $(\boldsymbol{z}_0, z_0^\theta)^{\mathrm{pr}} \in Z_H$,

$$\begin{aligned} z_{0,i}^{\mathrm{pr}}|_\gamma &= -\frac{1}{2}\left(\tau_{i,j}^{\mathrm{pr}}|_\gamma n_{\gamma,j}^{+} - \tau_{i,j}^{\mathrm{pr}}|_\gamma n_{\gamma,j}^{-}\right), \\ z_0^{\theta,\mathrm{pr}}|_\gamma &= -\frac{1}{2}\left(\tau_j^{\theta,\mathrm{pr}}|_\gamma n_{\gamma,j}^{+} - \tau_j^{\theta,\mathrm{pr}}|_\gamma n_{\gamma,j}^{-}\right), \end{aligned}$$

where $\boldsymbol{n}_\gamma^+$ (respectively $\boldsymbol{n}_\gamma^-$) denote the outward normal from the element on the arbitrarily chosen "positive" (respectively "negative") side of the edge γ, and

$$\begin{aligned} \tau_{i,j}^{\mathrm{pr}} &= \left(\frac{\partial u_{H,i}}{\partial x_j} + \frac{\partial u_{H,j}}{\partial x_i}\right) - p_H \delta_{ij} - u_{H,i} u_{H,j}, \\ \tau_j^{\theta,\mathrm{pr}} &= \frac{1}{\alpha}\frac{\partial \theta_H}{\partial x_j} - u_{H,j}\theta_H. \end{aligned}$$

Note that, since $u_{H,i}|_\gamma \in \mathbb{P}_2(\gamma)$, the approximation space for the hybrid flux includes quartic polynomials, $\mathbb{P}_4(\gamma)$, to correctly represent $z_{0,i}^{\mathrm{pr}}|_\gamma$ and $z_0^{\theta,\mathrm{pr}}|_\gamma$. An alternative approach is to interpolate the quartic term onto $\mathbb{P}_2$, and therefore use only $\mathbb{P}_2$ hybrid fluxes. For $(\boldsymbol{z}_0, z_0^\theta)^{\mathrm{du}}$, we obtain similar expressions

$$\begin{aligned} \tau_{i,j}^{\mathrm{du}} &= \left(\frac{\partial \psi_{Hi}}{\partial x_j} + \frac{\partial \psi_{Hj}}{\partial x_i}\right) - \lambda_H \delta_{ij}, \\ \tau_j^{\theta,\mathrm{du}} &= \frac{1}{\alpha}\frac{\partial \mu_H}{\partial x_j}. \end{aligned}$$

Now, to satisfy Eqs. (19) and (20), we correct these initial approximations as follows:

$$
\begin{aligned}
(\boldsymbol{z}, z^\theta)^{\mathrm{pr}} &= (\boldsymbol{z}_0, z_0^\theta)^{\mathrm{pr}} + (\boldsymbol{z}_l, z_l^\theta)^{\mathrm{pr}} + (\boldsymbol{z}_q, z_q^\theta)^{\mathrm{pr}},\\
(\boldsymbol{z}, z^\theta)^{\mathrm{du}} &= (\boldsymbol{z}_0, z_0^\theta)^{\mathrm{du}} + (\boldsymbol{z}_l, z_l^\theta)^{\mathrm{du}} + (\boldsymbol{z}_q, z_q^\theta)^{\mathrm{du}},
\end{aligned}
$$

where $(\boldsymbol{z}_l, z_l^\theta)^{\mathrm{pr}}$ and $(\boldsymbol{z}_l, z_l^\theta)^{\mathrm{du}}$ are $\mathbb{P}_1$ corrections, and $(\boldsymbol{z}_q, z_q^\theta)^{\mathrm{pr}}$ and $(\boldsymbol{z}_q, z_q^\theta)^{\mathrm{du}}$ are $\mathbb{P}_2$ corrections. To obtain these corrections, we adapt a procedure developed in the context of energy-norm implicit Neumann subproblems indicators [7, 2, 10].

2.3.4 Step 4

We first compute the "incompressible local projections", $(\tilde{\boldsymbol{u}}_H, \tilde{p}_H, \tilde{\theta}_H) \in Y_h$ for the primal problem, and $(\tilde{\boldsymbol{\psi}}_H, \tilde{\lambda}_H, \tilde{\mu}_H) \in Y_h$ for the dual problem. These projections are constructed to satisfy the following constraints on the fine mesh

$$
b(\tilde{\boldsymbol{u}}_H, q) = 0, \quad \forall q \in M_h, \tag{21}
$$

$$
b(\tilde{\boldsymbol{\psi}}_H, q) = -L((\boldsymbol{u}_H, p_H, \theta_H); (\mathbf{0}, q, 0)), \quad \forall q \in M_h, \tag{22}
$$

which eliminates the indefinite terms associated with the incompressibility constraint. We choose $\tilde{\theta}_H = \theta_H$, and, to satisfy Eq. (21), we write $(\tilde{\boldsymbol{u}}_H, \tilde{p}_H) = (\boldsymbol{u}_H, p_H) + (\boldsymbol{\Delta}_h, \delta_h)$, where, for all $T_H \in \mathcal{T}_H$, we have $(\boldsymbol{\Delta}_h|_{T_H}, \delta_h|_{T_H}) \in X_{T_H} \times M_{T_H}$ solution of

$$
\begin{aligned}
a_{T_H}(\boldsymbol{\Delta}_h|_{T_H}, \boldsymbol{v}) + b_{T_H}(\boldsymbol{v}, \delta_h|_{T_H}) &= 0, \quad \forall \boldsymbol{v} \in X_{T_H},\\
b_{T_H}(\boldsymbol{\Delta}_h|_{T_H}, q) &= -b(\boldsymbol{u}_H|_{T_H}, q), \quad \forall q \in M_{T_H}.
\end{aligned}
$$

with

$$
a_{T_H}(\boldsymbol{v}, \boldsymbol{w}) = \int_{T_H} \frac{\partial v_i}{\partial x_j} \frac{\partial w_i}{\partial x_j}\, d\Omega, \quad b_{T_H}(\boldsymbol{v}, r) = -\int_{T_H} \frac{\partial v_i}{\partial x_i} r\, d\Omega,
$$

and

$$
\begin{aligned}
X_{T_H} =& \{\boldsymbol{v} \in H_0^1(T_H) \times H_0^1(T_H) \,|\, v_i|_{T_h} \in \mathbb{P}_2(T_h) \oplus B_3(T_h), \forall T_h \in \mathcal{T}_h\},\\
M_{T_H} =& \{p \in L^2(T_H) \,|\, p|_{T_h} \in \mathbb{P}_1(T_h), \forall T_h \in \mathcal{T}_h\}.
\end{aligned}
$$

This problem is solvable since $b(\boldsymbol{u}_H|_{T_H}, 1) = b(\boldsymbol{u}_H, 1|_{T_H}) = 0$ for all $T_H \in \mathcal{T}_H$ thanks to the discontinuous pressure space.

Similarly, we choose $\tilde{\mu}_H = \mu_H$ and, to satisfy Eq. (22), we write $(\tilde{\boldsymbol{\psi}}_H, \tilde{\mu}_H) = (\boldsymbol{\psi}_H, \mu_H) + (\boldsymbol{\Delta}_h, \delta_h)$, where, for all $T_H \in \mathcal{T}_H$, we have $(\boldsymbol{\Delta}_h|_{T_H}, \delta_h|_{T_H}) \in X_{T_H} \times M_{T_H}$ solution of

$$a_{T_H}(\boldsymbol{\Delta}_h|_{T_H}, \boldsymbol{v}) + b_{T_H}(\boldsymbol{v}, \delta_h|_{T_H}) = 0, \quad \forall \boldsymbol{v} \in X_{T_H},$$
$$b_{T_H}(\boldsymbol{\Delta}_h|_{T_H}, q) = -b(\boldsymbol{\psi}_H|_{T_H}, q) - L((\boldsymbol{u}_H, p_H, \theta_H); (\mathbf{0}, q, 0)), \quad \forall q \in M_{T_H}.$$

These equations form a solvable system since, from Eq. (18),

$$b(\boldsymbol{\psi}_H, 1|_{T_H}) = -L((\boldsymbol{u}_H, p_H, \theta_H); (\mathbf{0}, 1|_{T_H}, 0)).$$

A priori estimates for the projections $\tilde{\boldsymbol{u}}_H$ and $\tilde{\boldsymbol{\psi}}_H$ are derived in Appendix 1.

We now compute the primal and dual "reconstructed errors", $(\hat{\boldsymbol{e}}, \hat{\varepsilon}, \hat{e}^\theta)^{\mathrm{pr}} \in \hat{Y}_h$ and $(\hat{\boldsymbol{e}}, \hat{\varepsilon}, \hat{e}^\theta)^{\mathrm{du}} \in \hat{Y}_h$, which satisfy the following equations

$$2E_0((\hat{\boldsymbol{e}}, \hat{\varepsilon}, \hat{e}^\theta)^{\mathrm{pr}}, (\boldsymbol{v}, q, \phi)) = \mathcal{R}^{\mathrm{pr}}((\tilde{\boldsymbol{u}}_H, \tilde{p}_H, \tilde{\theta}_H); (\boldsymbol{v}, q, \phi)) - B((\boldsymbol{v}, \phi), (\boldsymbol{z}, z^\theta)^{\mathrm{pr}}), \quad \forall (\boldsymbol{v}, q, \phi) \in \hat{Y}_h, \quad (23)$$

and

$$2E_0((\hat{\boldsymbol{e}}, \hat{\varepsilon}, \hat{e}^\theta)^{\mathrm{du}}), (\boldsymbol{v}, q, \phi)) = \mathcal{R}^{\mathrm{du}}((\boldsymbol{u}_H, p_H, \theta_H); (\tilde{\boldsymbol{\psi}}_H, \tilde{\lambda}_H, \tilde{\mu}_H); (\boldsymbol{\psi}_H, \mu_H); (\boldsymbol{v}, q, \phi)) - B((\boldsymbol{v}, \phi), (\boldsymbol{z}, z^\theta)^{\mathrm{du}}), \quad \forall (\boldsymbol{v}, q, \phi) \in \hat{Y}_h. \quad (24)$$

According to our definition of the space $\hat{Y}_h$ correspond to local (elemental) decoupled Neumann problems; the solvability of these subproblems is discussed in Appendix 2. Note that both the incompressible projection and the Neumann subproblems are local and linear, and, therefore, are inexpensive to compute compared to the global fine mesh problem, Eq. (10). This issue is further discussed in Section 4.

2.3.5 Step 5

Finally, we compute the bounds, $s_H^\pm$, according to

$$s_H^\pm = S(\tilde{\boldsymbol{u}}_H, \tilde{p}_H, \tilde{\theta}_H) - \mathcal{R}^{\mathrm{pr}}((\tilde{\boldsymbol{u}}_H, \tilde{p}_H, \tilde{\theta}_H); (\tilde{\boldsymbol{\psi}}_H, \tilde{\mu}_H, \tilde{\lambda}_H)) \pm \kappa^u E_0((\hat{\mathbf{e}}^\pm, \hat{\varepsilon}^\pm, 0); (\hat{\mathbf{e}}^\pm, \hat{\varepsilon}^\pm, 0)) \pm \kappa^\theta E_0((\mathbf{0}, 0, \hat{e}^{\theta,\pm}); (\mathbf{0}, 0, \hat{e}^{\theta,\pm})) \quad (25)$$

where

$$(\hat{\mathbf{e}}^{\pm}, \hat{\varepsilon}^{\pm}, \hat{e}^{\theta,\pm}) = (\hat{\mathbf{e}}, \hat{\varepsilon}, \hat{e}^{\theta})^{\mathrm{pr}} \mp \frac{1}{\kappa^u}(\hat{\mathbf{e}}, \hat{\varepsilon}, 0)^{\mathrm{du}} \mp \frac{1}{\kappa^{\theta}}(\mathbf{0}, 0, \hat{e}^{\theta})^{\mathrm{du}}. \tag{26}$$

In this expression, κ^u and κ^θ are two strictly positive reals. The choice of these parameters will affect the half bound gap

$$\begin{aligned}
\Delta_H &\equiv \frac{1}{2}(s_H^+ - s_H^-) \\
&= \kappa^u E_0((\hat{\mathbf{e}}, \hat{\varepsilon}, 0)^{\mathrm{pr}}, (\hat{\mathbf{e}}, \hat{\varepsilon}, 0)^{\mathrm{pr}}) + \frac{1}{\kappa^u} E_0((\hat{\mathbf{e}}, \hat{\varepsilon}, 0)^{\mathrm{du}}, (\hat{\mathbf{e}}, \hat{\varepsilon}, 0)^{\mathrm{du}}) \\
&+ \kappa^\theta E_0((\mathbf{0}, 0, \hat{e}^{\theta})^{\mathrm{pr}}, (\mathbf{0}, 0, \hat{e}^{\theta})^{\mathrm{pr}}) + \frac{1}{\kappa^\theta} E_0((\mathbf{0}, 0, \hat{e}^{\theta})^{\mathrm{du}}, (\mathbf{0}, 0, \hat{e}^{\theta})^{\mathrm{du}}).
\end{aligned}$$

Since $(\hat{\mathbf{e}}, \hat{\varepsilon}, \hat{e}^{\theta})^{\mathrm{pr}}$ and $(\hat{\mathbf{e}}, \hat{\varepsilon}, \hat{e}^{\theta})^{\mathrm{du}}$ do not depend on the choice of κ^u and κ^θ, we can readily find κ^u and κ^θ which minimize the bound gap, and hence renders the lower and upper bound as sharp as possible. This procedure gives

$$\begin{aligned}
\kappa^u &= \sqrt{\frac{E_0((\hat{\mathbf{e}}, \hat{\varepsilon}, 0)^{\mathrm{du}}, (\hat{\mathbf{e}}, \hat{\varepsilon}, 0)^{\mathrm{du}})}{E_0((\hat{\mathbf{e}}, \hat{\varepsilon}, 0)^{\mathrm{pr}}, (\hat{\mathbf{e}}, \hat{\varepsilon}, 0)^{\mathrm{pr}})}}, \\
\kappa^\theta &= \sqrt{\frac{E_0((\mathbf{0}, 0, \hat{e}^{\theta})^{\mathrm{du}}, (\mathbf{0}, 0, \hat{e}^{\theta})^{\mathrm{du}})}{E_0(\mathbf{0}, 0, \hat{e}^{\theta})^{\mathrm{pr}}, (\mathbf{0}, 0, \hat{e}^{\theta})^{\mathrm{pr}})}}.
\end{aligned}$$

2.4 Bounding Properties

If we define the errors $\tilde{\mathbf{e}} = \boldsymbol{u}_h - \tilde{\boldsymbol{u}}_H$, $\tilde{\varepsilon} = p_h - \tilde{p}_H$, and $\tilde{e}^\theta = \theta_h - \tilde{\theta}_H$, we can derive the following bound error expression,

$$s_H^{\pm} = s_h \pm D^{\pm} + I^{\pm}, \tag{27}$$

where

$$D^{\pm} = \kappa^u \mathcal{F}_0(\tilde{\mathbf{e}} - \hat{\mathbf{e}}^{\pm}, \tilde{\varepsilon} - \hat{\varepsilon}^{\pm}, 0) + \kappa^\theta \mathcal{F}_0(\mathbf{0}, 0, \tilde{e}^\theta - \hat{e}^{\theta,\pm}), \tag{28}$$

with $\mathcal{F}_0(\boldsymbol{v}, q, \phi) = E_0((\boldsymbol{v}, q, \phi), (\boldsymbol{v}, q, \phi))$. Recall that $s_h = S(\boldsymbol{u}_h, p_h, \theta_h)$ is the fine mesh ("truth") output. The derivation of the bound error expression and the definition of $I^{\pm}$ are given in Appendix 3.

We now show that $D^{\pm} \geq 0$. We have $\mathcal{F}_0(\mathbf{0}, 0, \tilde{e}^\theta - \hat{e}^\theta) \geq 0$ since, for all $\phi \in X_h^\theta$, $\mathcal{F}_0(\mathbf{0}, 0, \phi) = a^\theta(\phi, \phi) \geq 0$. Moreover, using the definition of E_0, Eq. (13), we can write

$$\mathcal{F}_0(\tilde{\mathbf{e}} - \hat{\mathbf{e}}^{\pm}, \tilde{\varepsilon} - \hat{\varepsilon}^{\pm}, 0) = a(\tilde{\mathbf{e}} - \hat{\mathbf{e}}^{\pm}, \tilde{\mathbf{e}} - \hat{\mathbf{e}}^{\pm}) + 2b(\tilde{\mathbf{e}} - \hat{\mathbf{e}}^{\pm}, \tilde{\varepsilon} - \hat{\varepsilon}^{\pm}). \tag{29}$$

For all $q \in M_h$, we have, from (23) and (24), taking $(\boldsymbol{v}, q, \phi) = (\boldsymbol{0}, q, 0)$,

$$2\kappa^u b(\hat{\boldsymbol{e}}^{\pm}, q) = -\kappa^u b(\tilde{\boldsymbol{u}}_H, q) \pm [b(\tilde{\boldsymbol{\psi}}_H, q) + L((\boldsymbol{u}_H, p_H, \theta_H); (\boldsymbol{0}, q, 0))],$$

and, by virtue of Eqs. (21) and (22), we find that $2\kappa^u b(\hat{\boldsymbol{e}}^{\pm}, q) = 0$ and $b(\tilde{\boldsymbol{e}}, q) = b(\boldsymbol{u}_h - \tilde{\boldsymbol{u}}_H, q) = 0$, $\forall q \in M_h$; therefore,

$$\mathcal{F}_0(\tilde{\boldsymbol{e}} - \hat{\boldsymbol{e}}^{\pm}, \tilde{\varepsilon} - \hat{\varepsilon}^{\pm}, 0) = a(\tilde{\boldsymbol{e}} - \hat{\boldsymbol{e}}^{\pm}, \tilde{\boldsymbol{e}} - \hat{\boldsymbol{e}}^{\pm}) \geq 0.$$

We now examine the bound error expression, Eq. (27), and we see that the upper bound, (respectively the lower bound), departs from the "truth", s_h, by a positive (respectively negative) definite contribution D^+ (respectively D^-), and an indefinite contribution I^+ (respectively I^-). The essential point is that $D^{\pm}$ involves gradients only, and is expected to converge at best like H^4 [10]. More precisely, we assume that there is a positive constant, $C_D > 0$, such that $C_D H^4 \leq D^{\pm}$ — a variant of the method, based on a hypothesis easier to verify, is introduced in [16]. As argued in Appendix 4, the indefinite contribution $I^{\pm}$ involves only weaker norms and converges like H^5, that is there exists a positive constant C_I such that $I^{\pm} \leq C_I H^5$. Therefore, if we define $H^* = C_D/C_I$, according to Eq. (27) we obtain bounds for all $H < H^*$. The numerical examples presented hereafter will show that bounds are in practice always obtained provided the mesh even barely resolves the flow. This issue will be further discussed in Section 4.

3 Numerical Examples

We first present numerical results for natural convection in a square domain. The problem is defined by Eqs. (1), (2), and (3), the geometry of the problem is shown in Fig. 2(a), and the boundary conditions are $\boldsymbol{u}|_{\partial\Omega} = 0$, $\theta = 0$ on Γ_0, $\frac{\partial \theta}{\partial n} = 1$ on Γ_I, and $\frac{\partial \theta}{\partial n} = 0$ otherwise. The Prandtl number and the Grashof number are $\alpha = 1$ and $\beta = 30,000$. For this choice of parameters, the Nusselt number is $\mathrm{Nu} = 2.49$ ($\mathrm{Nu}^{-1} = \frac{1}{\Gamma_I} \int_{\Gamma_I} \theta_h \, ds$, computed with the fine mesh solution); for a pure conduction problem in this geometry, $\mathrm{Nu} = 1$, and thus $\mathrm{Nu} = 2.49$ indicates the existence of velocity and thermal boundary layers near Γ_I and Γ_0. The elements of the coarsest mesh, $\mathcal{T}_{H_0}$, are chosen so that the diameter of the mesh, H_0, is approximately the size of the thickness of the boundary layers. Figures 2(b), 2(c), and 2(d) represent the fine mesh $\mathcal{T}_h$, the streamlines, and the isotherms obtained on the fine mesh.

Figures 3(a) and 3(b) show the convergence of the bounds for the nonlinear output,

$$S_1(\boldsymbol{u}, p, \theta) = \int_{\Omega} |\boldsymbol{u}|^2 \, dA,$$

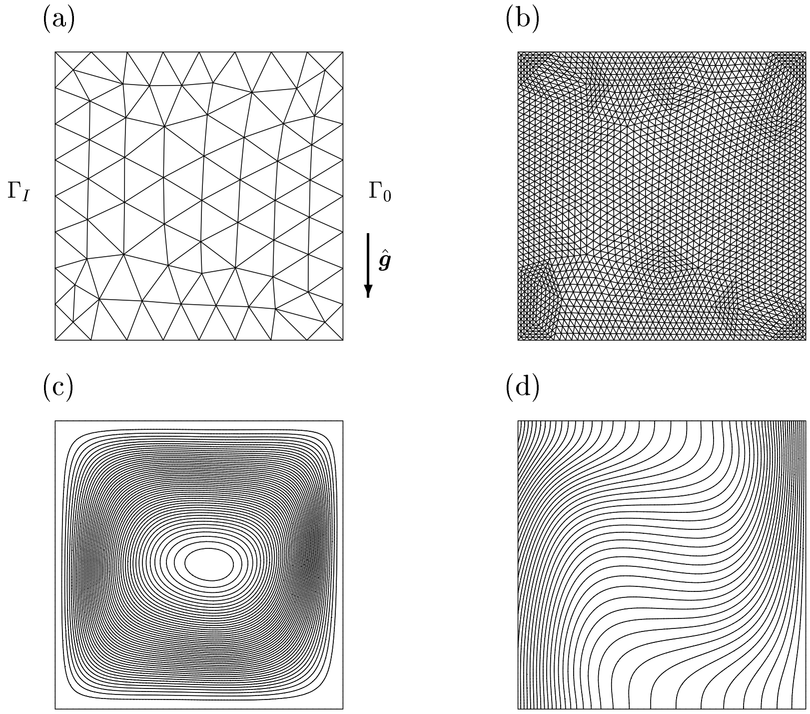

Figure 2: (a) Domain and coarse mesh, $\mathcal{T}_{H_0}$. (b) Fine "truth" mesh, $\mathcal{T}_h$. (c) Streamlines. (d) Isotherms.

corresponding to the kinetic energy of the flow. In Fig. 3(a), we have represented the normalized lower and upper bounds s_H^+/s_h and s_H^-/s_h, and the normalized "coarse" mesh output, s_H/s_h, for different meshes $\mathcal{T}_H$. The mesh diameters vary from $H = H_0$ to $H = H_0/6$; $\mathcal{T}_h = \mathcal{T}_{H_0/6}$ is the fine mesh. For this problem, bounds have been observed on all the meshes considered. Figure 3(b) demonstrates that the convergence rate of the bound gap is optimal, $O(H^4)$; the measured effectivity factor η, defined as $\eta = \Delta_H/|s_h - s_H|$, is $7.3 \leq \eta \leq 7.7$.

Similar results are obtained for the output

$$S_2(\boldsymbol{u}, p, \theta) = \frac{1}{|\Gamma_I|}\int_{\Gamma_I} \theta \, ds.$$

Figures 3(c) and 3(d) show the convergence of the bounds and of the bound gap; again optimality is achieved. For this output the effectivity factor is $3.6 \leq \eta \leq 5$.

We next present results obtained for the model problem defined by Eqs. (1), (2) and (3), the boundary conditions (4), and the domain represented in Fig. 1(a). The output of interest is

$$S(\boldsymbol{u}, p, \theta) = \frac{1}{|\Gamma_1|}\int_{\Gamma_1} \theta \, d\Gamma.$$

For this case the (nondimensional) heat flux is $q = 1$, and the Prandtl and Grashof numbers are $\alpha = 1$ and $\beta = 50,000$; the resulting streamlines are shown in Fig. 4(a).

Since the cost of computing the bounds is essentially a function of the number of elements T_H in $\mathcal{T}_H$, it is desirable to construct optimized triangulations that maximize the bound accuracy (minimize the bound gap) for a given number of degrees of freedom. As shown in [17], the bound gap, Δ_H, can be expressed as a sum of local elemental positive contributions: $\Delta_H = \sum_{T_H \in \mathcal{T}_H} \Delta_{T_H}$, with $\Delta_{T_H} \geq 0$. We can, therefore, implement a simple adaptive strategy. Starting from an initial grid, $\mathcal{T}_H^0$, with bound gap Δ_H^0, we generate a sequence of triangulations $\{\mathcal{T}_H^k, k = 1, 2, ...\}$ with corresponding bound gaps $\{\Delta_H^k, k = 1, 2, ...\}$, such that each triangulation $\mathcal{T}_H^k$ is obtained by refinement of the selected triangles T_H^{k-1} such that $\Delta_{T_H}^{k-1} > \alpha \max_{T_H} \Delta_{T_H}^{k-1}$, for a specified parameter $0 < \alpha < 1$. The approach ensures that, for a sufficiently large k, $\Delta_H^k \leq \Delta_{\text{targ}}$, where $\Delta_{\text{targ}} > 0$ is a gap target.

The effectiveness of the adaptive procedure is summarized in Table 1, in which $\mathcal{T}_H^0$, $\mathcal{T}_H^{k_1}$, and $\mathcal{T}_H^{k_2}$ denotes successive adapted meshes corresponding to

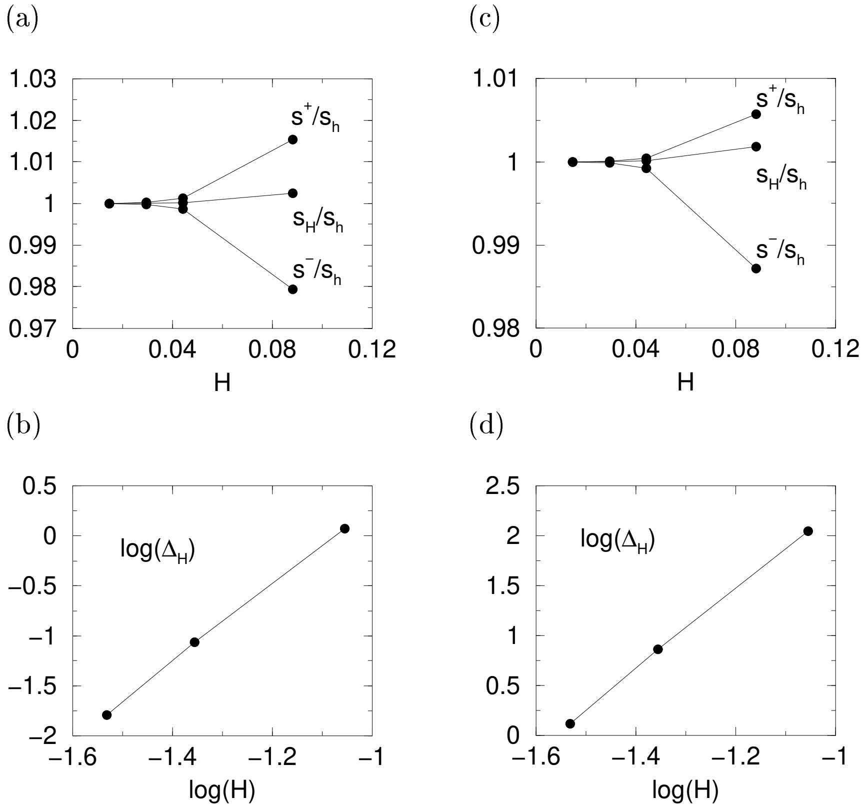

Figure 3: Convergence of the (normalized) bounds $s_H^{\pm}/s_h$, for (a) the kinetic energy, S_1, and (c) the mean temperature on the heated boundary, S_2. Figures 3(b) and 3(d) show the convergence of the bound gap, Δ_H, for S_1 and S_2, respectively .

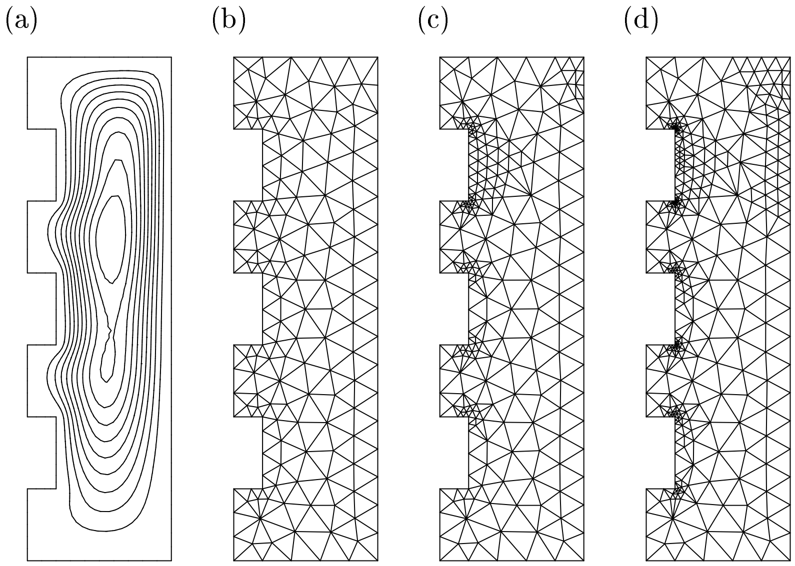

Figure 4: Model problem. (a) Streamlines. (b) Mesh $\mathcal{T}_H^0$. (c) Mesh $\mathcal{T}_H^{k_1}$. (d) Mesh $\mathcal{T}_H^{k_2}$.

	$\mathcal{T}_H$	$\mathcal{T}_H^{k_1}$	$\mathcal{T}_H^{k_2}$	$\mathcal{T}_{H/2}$
# of elements	264	416	628	1056
s^-	0.253	0.270	0.273	0.272
s^+	0.296	0.282	0.279	0.279
Δ_H	0.0212	0.0057	0.0026	0.0036

Table 1: Convergence of the bounds for problem of Fig. 1(a).

Figures 4(b), (c) and (d), respectively; the mesh $\mathcal{T}_{H/2}$ is a *uniform* refinement of $\mathcal{T}_H^0$. Table 1 shows that a reduction of the relative bound gap from $\approx 8\%$ for mesh $\mathcal{T}_H^0$ to less than 1% for mesh $\mathcal{T}_H^{k_2}$ is achieved by optimal refinement with a final mesh which contains only slightly more than twice the number of elements of the mesh $\mathcal{T}_H^0$. Note that, for each of the adapted coarse meshes, the "truth" fine mesh is obtained by dividing each element of the adapted coarse mesh into 6^2 elements, implying that the truth mesh is also adapted; nevertheless, our choice of a conservative initial fine mesh guarantees that the truth solution is insensitive to the adaptation of the fine mesh.

4 Attributes of the method

We review here the four attributes of the method defined in the Introduction.

4.1 Attribute A1

To summarize the previous discussion, we have shown that bounds are obtained for all mesh diameter $H < H^*$, where H^* is an (unknown) threshold. Note that we expect the singular perturbation prefactors, $1/\alpha$ and $1/\beta$ (recall that α and β are the Prandtl and the Grashof number), to unfortunately favor the indefinite terms; nevertheless, the corresponding *numerical* singular perturbation parameter will be small as soon as the coarse space even roughly resolves the structure of the solution, and thus the bound property will be preserved except perhaps on very crude meshes.

We conclude that, even if H^* is not known *a priori*, bounds are obtained once the solution is marginally resolved. In numerical examples, we have always observed bounds, and thus the uncertainty associated with H^* is not an important practical issue, though it constitutes a real theoretical issue. Note that H^* is a threshold parameter (bounds are obtained for all $H < H^*$); therefore, even if H^* is not known, the method presents a significant advantage over previous explicit *a posteriori* estimation procedures in which the estimators themselves involve unknown constants and functions. Note also that, for linear coercive problems, bounds are obtained for any H ($H^* = \infty$) [14, 15, 17].

There is another source of uncertainty, namely the choice of the fine mesh $\mathcal{T}_h$, which should be selected fine enough to ensure that $|s - s_h|$ is negligible (recall that s is the exact solution). In practice, the mesh $\mathcal{T}_h$ is chosen conservatively by estimating *a priori* the size of the smallest structure anticipated and ensuring that $\mathcal{T}_h$ provides for an accurate representation of such structures.

4.2 Attribute A2

The bounds are sharp. As demonstrated by the numerical results, the bound gap converges at an optimal rate; for sufficiently regular problems we have observed $\Delta_H \leq CH^4$. The effectivity factor, $\eta = \Delta_H/|s_h - s_H|$, has also been measured, typically $1 \leq \eta \leq 10$, though this will be problem — and output — dependent.

4.3 Attribute A3

We have used the local decomposition of the bound gap into elemental positive contributions to implement an adaptive refinement strategy. We have shown that a straightforward implementation yields a very efficient procedure which allows us to obtain a threshold error on the output with an optimal number of finite elements.

4.4 Attribute A4

We recall that $(\boldsymbol{u}_h, p_h, \theta_h)$ and $s_h = S(\boldsymbol{u}_h, p_h, \theta_h)$ are the field variables and the output that are effectively indistinguishable from the truth — and correspondingly expensive. Our lower and upper bounds are only interesting if they can be obtained at considerably less expense than computation of s_h — and preferably at only slightly greater expense than computation of s_H, the coarse approximation. From our definitions of Y_h and $\hat{Y}_h$, we see that Eqs. (23) and (24) correspond to many local, uncoupled, small, Neumann subproblems, whereas Eq. (10) corresponds to a single, large, global problem. It follows that Eqs. (23) and (24) present a smaller bandwidth — yielding substantial savings in both memory and computational time of direct solution strategies — and a smaller condition number — yielding faster convergence in iterative methods. In addition, Eqs. (23) and (24) are symmetric, positive definite, and completely decoupled — the latter enabling straightforward parallel implementations. Furthermore, the dual problem, Eq. (18), and the subproblems, Eqs. (23) and (24), are linear, leading to additional savings compared to the original nonlinear fine mesh problem. The relative savings are, of course, reduced as the global solver improves.

Appendices

1 "Incompressible Projection"

We write $(\tilde{\boldsymbol{u}}_H, \tilde{p}_H) = (\boldsymbol{u}_H, p_H) + (\boldsymbol{\Delta}_h, \delta_H)$, where for all $T_H \in \mathcal{T}_H$, we have $(\boldsymbol{\Delta}_h|_{T_H}, \delta_h|_{T_H}) \in X_{T_H} \times M_{T_H}$ that satisfies

$$a_{T_H}(\boldsymbol{\Delta}_h|_{T_H}, \boldsymbol{v}) + b_{T_H}(\boldsymbol{v}, \delta_h|_{T_H}) = 0, \qquad \forall \boldsymbol{v} \in X_{T_H}, \tag{30}$$

$$b_{T_H}(\boldsymbol{\Delta}_h|_{T_H}, q) = -b(\boldsymbol{u}_H|_{T_H}, q) \qquad \forall q \in M_{T_H}. \tag{31}$$

This problem is solvable since $b(\boldsymbol{u}_H|_{T_H}, 1) = b(\boldsymbol{u}_H, 1|_{T_H}) = 0$ for all $T_H \in \mathcal{T}_H$.

Given any $T_H \in \mathcal{T}_H$, we first note that the inf-sup parameter, β_{T_H}, for Eqs. (30) and (31) is independent of h and independent of H (β_{T_H} depends only on the shape of T_H but not on its size); the latter follows from the scale invariance of β_{T_H} when defined with respect to the $H^1(T_H)$ seminorm (which is equivalent to the $H^1(T_H)$ norm as we have Dirichlet conditions on ∂T_H). Therefore, $\exists \boldsymbol{v} \in X_{T_H}$, such that

$$\begin{aligned}\beta_{T_H}|\boldsymbol{v}|_{H^1(T_H)}||\delta_h||_{L^2(T_H)} \leq |b_{T_H}(\boldsymbol{v}, \delta_h|_{T_H})| &= |a_{T_H}(\boldsymbol{\Delta}_h|_{T_H}, \boldsymbol{v})| \\ &\leq |\boldsymbol{\Delta}_h|_{H^1(T_H)}|\boldsymbol{v}|_{H^1(T_H)},\end{aligned}$$

thus

$$||\delta_h||_{L^2(T_H)} \leq \frac{1}{\beta_{T_H}}|\boldsymbol{\Delta}_h|_{H^1(T_H)}.$$

We then note that

$$\begin{aligned}a_{T_H}(\boldsymbol{\Delta}_h, \boldsymbol{\Delta}_h) = |\boldsymbol{\Delta}_h|^2_{H^1(T_H)} &= -b_{T_H}(\boldsymbol{\Delta}_h, \delta_h) = b(\boldsymbol{u}_H|_{T_H}, \delta_h) \\ &= -b(\boldsymbol{u}_h|_{T_H} - \boldsymbol{u}_H|_{T_H}, \delta_h) \\ &\leq C|\boldsymbol{u}_h - \boldsymbol{u}_H|_{H^1(T_H)}||\delta_h||_{L^2(T_H)} \\ &\leq \frac{C}{\beta_{T_H}}|\boldsymbol{u}_h - \boldsymbol{u}_H|_{H^1(T_H)}|\boldsymbol{\Delta}_h|_{H^1(T_H)}.\end{aligned}$$

Therefore, we have, for all $T_H \in \mathcal{T}_H$,

$$|\boldsymbol{\Delta}_h|_{H^1(T_H)} \leq \frac{C}{\beta_{T_H}}|\boldsymbol{u}_h - \boldsymbol{u}_H|_{H^1(T_H)};$$

moreover, since $\boldsymbol{\Delta}_h|_{\partial T_H} = 0$, we can apply the Poincaré inequality in conjunction with a scaling argument to find

$$||\boldsymbol{\Delta}_h||_{L^2(T_H)} \leq \frac{C}{\beta_{T_H}}H|\boldsymbol{u}_h - \boldsymbol{u}_H|_{H^1(T_H)}.$$

Finally, squaring and summing over all $T_H \in \mathcal{T}_H$ yields the estimates

$$\begin{aligned}|\tilde{\boldsymbol{u}}_H - \boldsymbol{u}_H|_{H^1(\Omega)} &\leq C|\boldsymbol{u}_h - \boldsymbol{u}_H|_{H^1(\Omega)}, \\ ||\tilde{\boldsymbol{u}}_H - \boldsymbol{u}_H||_{L^2(\Omega)} &\leq CH|\boldsymbol{u}_h - \boldsymbol{u}_H|_{H^1(\Omega)}.\end{aligned}$$

The procedure for $(\tilde{\boldsymbol{\psi}}_H, \tilde{\lambda}_H)$ is identical except that the right-hand-side in Eq. (31) is now $-b(\boldsymbol{\psi}_H|_{T_H}, q) - L((\boldsymbol{u}_H, p_H, \tilde{\theta}_H); (\mathbf{0}, q, 0))$. If we denote $\boldsymbol{\psi}_h$, the adjoint obtained on the fine mesh, then we have

$$b(\boldsymbol{\psi}_h|_{T_H}, q) = -L((\boldsymbol{u}_H, p_H, \tilde{\theta}_H); (\mathbf{0}, q, 0)), \quad \forall q \in M_{T_H};$$

therefore,

$$a_{T_H}(\boldsymbol{\Delta}_h, \boldsymbol{\Delta}_h) = -b_{T_H}(\boldsymbol{\psi}_h - \boldsymbol{\psi}_H, \delta_h),$$

and the rest of the proof follows. We thus obtain the estimates

$$|\tilde{\boldsymbol{\psi}}_H - \boldsymbol{\psi}_H|_{H^1(\Omega)} \leq C|\boldsymbol{\psi}_h - \boldsymbol{\psi}_H|_{H^1(\Omega)},$$
$$||\tilde{\boldsymbol{\psi}}_H - \boldsymbol{\psi}_H||_{L^2(\Omega)} \leq CH|\boldsymbol{\psi}_h - \boldsymbol{\psi}_H|_{H^1(\Omega)}.$$

2 Solvability of the Local Neumann Subproblems

To ensure solvability of Eqs. (23) and (24), we must prove

$$\mathcal{R}^{\mathrm{pr}}(\tilde{\boldsymbol{u}}_H, \tilde{p}_H, \tilde{\theta}_H); (\boldsymbol{v}^s, q^s, \phi^s)) = B((\boldsymbol{v}^s, \phi^s), (\boldsymbol{z}, z^\theta)^{\mathrm{pr}}),$$

and

$$\mathcal{R}^{\mathrm{du}}((\boldsymbol{u}_H, p_H, \theta_H); (\tilde{\boldsymbol{\psi}}_H, \tilde{\lambda}_H, \tilde{\mu}_H); (\boldsymbol{\psi}_H, \mu_H); (\boldsymbol{v}^s, q^s, \phi^s)) = \\ B((\boldsymbol{v}^s, \phi^s), (\boldsymbol{z}, z^\theta)^{\mathrm{du}}),$$

for all the singular modes $(\boldsymbol{v}^s, q^s, \phi^s) \in \hat{Y}_h$ defined by

$$E_0((\boldsymbol{w}, r, \rho), (\boldsymbol{v}^s, q^s, \phi^s)) = 0, \quad \forall (\boldsymbol{w}, r, \rho) \in \hat{Y}_h.$$

The velocity singular modes are $\boldsymbol{v}^s = (1|_{T_H}, 0), (0, 1|_{T_H}), (y|_{T_H}, -x|_{T_H})$, for all $T_H \in \mathcal{T}_H$, corresponding respectively to (elemental) translations in the x direction, translations in the y direction, and rotations. We also have the temperature modes $\phi^s = 1|_{T_H}$ and the pressure modes $q^s = 1|_{T_H}$. Since all these modes are in $\hat{Y}_H$, in view of Eqs. (19) and (20), we have to prove that

$$\mathcal{R}^{\mathrm{pr}}(\tilde{\boldsymbol{u}}_H, \tilde{p}_H, \tilde{\theta}_H); (\boldsymbol{v}^s, q^s, \phi^s)) = \mathcal{R}^{\mathrm{pr}}(\boldsymbol{u}_H, p_H, \theta_H); (\boldsymbol{v}^s, q^s, \phi^s)), \tag{32}$$

and

$$\mathcal{R}^{\mathrm{du}}((\boldsymbol{u}_H, p_H, \theta_H); (\tilde{\boldsymbol{\psi}}_H, \tilde{\lambda}_H, \tilde{\mu}_H); (\boldsymbol{\psi}_H, \mu_H); (\boldsymbol{v}^s, q^s, \phi^s)) = \\ \mathcal{R}^{\mathrm{du}}((\boldsymbol{u}_H, p_H, \theta_H); (\boldsymbol{\psi}_H, \lambda_H, \mu_H); (\boldsymbol{\psi}_H, \mu_H); (\boldsymbol{v}^s, q^s, \phi^s)). \tag{33}$$

Looking first at Eq. (32), we have that, by the definition of $\mathcal{R}^{\mathrm{pr}}$, Eq. (15),

$$\begin{aligned}\mathcal{R}^{\mathrm{pr}}((\tilde{\boldsymbol{u}}_H, \tilde{p}_H, \tilde{\theta}_H); (\boldsymbol{v}^s, 0, 0)) &= -\, a(\tilde{\boldsymbol{u}}_H, \boldsymbol{v}^s) - b(\boldsymbol{v}^s, \tilde{p}_H) \\ &\quad -\, c(\tilde{\boldsymbol{u}}_H, \tilde{\boldsymbol{u}}_H, \boldsymbol{v}^s) - d(\tilde{\theta}_H, \boldsymbol{v}^s) \\ &= -\, c(\tilde{\boldsymbol{u}}_H, \tilde{\boldsymbol{u}}_H, \boldsymbol{v}^s) - d(\tilde{\theta}_H, \boldsymbol{v}^s).\end{aligned}$$

Using the definition of c, and since the support of $\boldsymbol{v}^s$ is an element of $\mathcal{T}_H$, say T_H, we can write

$$\begin{aligned} c(\tilde{\boldsymbol{u}}_H, \tilde{\boldsymbol{u}}_H, \boldsymbol{v}^s) &= -\int_{T_H} \tilde{u}_{H,i}\tilde{u}_{H,j} \frac{\partial v_i^s}{\partial x_j}\, d\Omega \\ &= -\frac{1}{2}\int_{T_H} \tilde{u}_{H,i}\tilde{u}_{H,j} \left(\frac{\partial v_i^s}{\partial x_j} + \frac{\partial v_j^s}{\partial x_i}\right) d\Omega \\ &= 0, \end{aligned}$$

and we have, since the same argument applies to $c(\boldsymbol{u}_H, \boldsymbol{u}_H, \boldsymbol{v}^s)$ and since $\tilde{\theta}_H = \theta_H$,

$$\mathcal{R}^{\mathrm{pr}}((\tilde{\boldsymbol{u}}_H, \tilde{p}_H, \tilde{\theta}_H); (\boldsymbol{v}^s, 0, 0)) = \mathcal{R}^{\mathrm{pr}}((\boldsymbol{u}_H, p_H, \theta_H); (\boldsymbol{v}^s, 0, 0)).$$

We now consider

$$\begin{aligned} \mathcal{R}^{\mathrm{pr}}((\tilde{\boldsymbol{u}}_H, \tilde{p}_H, \tilde{\theta}_H); (\mathbf{0}, 0, \phi^s)) &= -a^\theta(\tilde{\theta}_H, \phi^s) - c^\theta(\tilde{\theta}_H, \tilde{\boldsymbol{u}}_H, \phi^s) - \langle g_N, \phi^s \rangle_N \\ &= -\langle g_N, \phi^s \rangle_N \\ &= \mathcal{R}^{\mathrm{pr}}((\boldsymbol{u}_H, p_H, \theta_H); (\mathbf{0}, 0, \phi^s)). \end{aligned}$$

Then, since for $q^s = 1|_{T_H}$,

$$\mathcal{R}^{\mathrm{pr}}((\tilde{\boldsymbol{u}}_H, \tilde{p}_H, \tilde{\theta}_H); (\mathbf{0}, q^s, 0)) = 0 = \mathcal{R}^{\mathrm{pr}}((\boldsymbol{u}_H, p_H, \theta_H); (\mathbf{0}, q^s, 0)),$$

Eq. (32) is satisfied.

Turning now to the dual problem, the definition of $\mathcal{R}^{\mathrm{du}}$, Eq. (16), gives

$$\begin{aligned} &\mathcal{R}^{\mathrm{du}}((\boldsymbol{u}_H, p_H, \theta_H); (\tilde{\boldsymbol{\psi}}_H, \tilde{\lambda}_H, \tilde{\mu}_H); (\boldsymbol{\psi}_H, \mu_H); (\boldsymbol{v}^s, q^s, \phi^s)) = \\ &\quad - L((\boldsymbol{u}_H, p_H, \theta_H); (\boldsymbol{v}^s, q^s, \phi^s)) - a(\tilde{\boldsymbol{\psi}}_H, \boldsymbol{v}^s) - a^\theta(\tilde{\mu}_h, \phi^s) \\ &\qquad\qquad - E_1((\boldsymbol{u}_H, \theta_H); (\boldsymbol{\psi}_H, \mu_H); (\boldsymbol{v}^s, \phi^s)). \end{aligned}$$

Since $a(\tilde{\boldsymbol{\psi}}_H, \boldsymbol{v}^s) = 0$ (and $a(\boldsymbol{\psi}_H, \boldsymbol{v}^s) = 0$)) and since $a^\theta(\tilde{\mu}_h, \phi^s) = 0$ (and $a^\theta(\mu_h, \phi^s) = 0$), Eq. (33) is satisfied.

3 Bound Error Expression

We define the errors $\tilde{\boldsymbol{e}} = \boldsymbol{u}_h - \tilde{\boldsymbol{u}}_H$, $\tilde{\varepsilon} = p_h - \tilde{p}_H$, and $\tilde{e}^\theta = \theta_h - \tilde{\theta}_H$. We note that, since $(\tilde{\boldsymbol{e}}, \tilde{\varepsilon}, \tilde{e}^\theta) \in Y_h$, then

$$B((\tilde{\boldsymbol{e}}, \tilde{e}^\theta), (\boldsymbol{z}, z^\theta)^{\mathrm{pr}}) = 0 \quad \text{and} \quad B((\tilde{\boldsymbol{e}}, \tilde{e}^\theta), (\boldsymbol{z}, z^\theta)^{\mathrm{du}}) = 0.$$

Therefore, from Eqs. (23) and (24), and from the definition of the form E_0, Eq. (13), we have

$$2E_0((\hat{\boldsymbol{e}},\hat{\varepsilon},0)^{\mathrm{pr}}),(\tilde{\boldsymbol{e}},\tilde{\varepsilon},0)) = \mathcal{R}^{\mathrm{pr}}(\tilde{\boldsymbol{u}}_H,\tilde{p}_H,\tilde{\theta}_H),(\tilde{\boldsymbol{e}},\tilde{\varepsilon},0)), \tag{34}$$

$$2E_0((\mathbf{0},0,\hat{e}^{\theta})^{\mathrm{pr}}),(\mathbf{0},0,\tilde{e}^{\theta})) = \mathcal{R}^{\mathrm{pr}}(\tilde{\boldsymbol{u}}_H,\tilde{p}_H,\tilde{\theta}_H),(\mathbf{0},0,\tilde{e}^{\theta})), \tag{35}$$

and similarly

$$\begin{aligned} 2E_0((\hat{\boldsymbol{e}},\hat{\varepsilon},\tilde{e}^{\theta})^{\mathrm{du}}),(\tilde{\boldsymbol{e}},\tilde{\varepsilon},\tilde{e}^{\theta})) &= \\ &\mathcal{R}^{\mathrm{du}}((\boldsymbol{u}_H,p_H,\theta_H);(\tilde{\boldsymbol{\psi}}_H,\tilde{\lambda}_H,\tilde{\mu}_H);(\boldsymbol{\psi}_H,\mu_H);(\tilde{\boldsymbol{e}},\tilde{\varepsilon},\tilde{e}^{\theta})). \end{aligned} \tag{36}$$

Then, using Eq. (26), we combine Eqs. (34), (35), and (36) to write

$$\begin{aligned} &2\kappa^u E_0((\hat{\boldsymbol{e}}^{\pm},\hat{\varepsilon}^{\pm},0));(\tilde{\boldsymbol{e}},\tilde{\varepsilon},0)) + 2\kappa^{\theta} E_0(\mathbf{0},0,\hat{e}^{\theta,\pm}));(\mathbf{0},0,\tilde{e}^{\theta})) = \\ &\quad \kappa^u \mathcal{R}^{\mathrm{pr}}(\tilde{\boldsymbol{u}}_H,\tilde{p}_H,\tilde{\theta}_H),(\tilde{\boldsymbol{e}},\tilde{\varepsilon},0)) + \kappa^{\theta}\mathcal{R}^{\mathrm{pr}}(\tilde{\boldsymbol{u}}_H,\tilde{p}_H,\tilde{\theta}_H),(\mathbf{0},0,\tilde{e}^{\theta})) \\ &\qquad \mp \mathcal{R}^{\mathrm{du}}((\boldsymbol{u}_H,p_H,\theta_H);(\tilde{\boldsymbol{\psi}}_H,\tilde{\lambda}_H,\tilde{\mu}_H);(\boldsymbol{\psi}_H,\mu_H);(\tilde{\boldsymbol{e}},\tilde{\varepsilon},\tilde{e}^{\theta})). \end{aligned} \tag{37}$$

We will now expand the right hand side of Eq. (37). Using Eq. (17), and the expansion, Eq. (12), one can write

$$\begin{aligned} \kappa^u \mathcal{R}^{\mathrm{pr}}(\tilde{\boldsymbol{u}}_H,\tilde{p}_H,\tilde{\theta}_H),(\tilde{\boldsymbol{e}},\tilde{\varepsilon},0)) &= \kappa^u E_0((\tilde{\boldsymbol{e}},\tilde{\varepsilon},\tilde{e}^{\theta}),(\tilde{\boldsymbol{e}},\tilde{\varepsilon},0)) \\ &+ \kappa^u E_1((\tilde{\boldsymbol{u}}_H,\tilde{\theta}_H);(\tilde{\boldsymbol{e}},\tilde{e}^{\theta}),(\tilde{\boldsymbol{e}},0)) + \kappa^u F((\tilde{\boldsymbol{e}},\tilde{e}^{\theta}),(\tilde{\boldsymbol{e}},\tilde{e}^{\theta}),(\tilde{\boldsymbol{e}},0)) \end{aligned} \tag{38}$$

and

$$\begin{aligned} \kappa^{\theta} \mathcal{R}^{\mathrm{pr}}(\tilde{\boldsymbol{u}}_H,\tilde{p}_H,\tilde{\theta}_H),(\mathbf{0},0,\tilde{e}^{\theta})) &= \kappa^{\theta} E_0((\tilde{\boldsymbol{e}},\tilde{\varepsilon},\tilde{e}^{\theta}),(\mathbf{0},0,\tilde{e}^{\theta})) \\ &+ \kappa^{\theta} E_1((\tilde{\boldsymbol{u}}_H,\tilde{\theta}_H);(\tilde{\boldsymbol{e}},\tilde{e}^{\theta}),(\mathbf{0},\tilde{e}^{\theta})) + \kappa^{\theta} F((\tilde{\boldsymbol{e}},\tilde{e}^{\theta}),(\tilde{\boldsymbol{e}},\tilde{e}^{\theta}),(\mathbf{0},\tilde{e}^{\theta})). \end{aligned} \tag{39}$$

From the definition of the dual residual, Eq. (16), we also have

$$\begin{aligned} &\mathcal{R}^{\mathrm{du}}((\boldsymbol{u}_H,p_H,\theta_H);(\tilde{\boldsymbol{\psi}}_H,\tilde{\lambda}_H,\tilde{\mu}_H);(\boldsymbol{\psi}_H,\mu_H);(\tilde{\boldsymbol{e}},\tilde{\varepsilon},\tilde{e}^{\theta})) = \\ &\qquad - L((\boldsymbol{u}_H,p_H,\theta_H);(\tilde{\boldsymbol{e}},\tilde{\varepsilon},\tilde{e}^{\theta})) - E_0((\tilde{\boldsymbol{\psi}}_H,\tilde{\lambda}_H,\tilde{\mu}_H),(\tilde{\boldsymbol{e}},\tilde{\varepsilon},\tilde{e}^{\theta})) \\ &\qquad\qquad - E_1((\boldsymbol{u}_H,\theta_H);(\boldsymbol{\psi}_H,\mu_H),(\tilde{\boldsymbol{e}},\tilde{\varepsilon})), \end{aligned}$$

which, by virtue of Eqs. (17) and (12), can be rewritten

$$\begin{aligned} &\mathcal{R}^{\mathrm{du}}((\boldsymbol{u}_H,p_H,\theta_H);(\tilde{\boldsymbol{\psi}}_H,\tilde{\lambda}_H,\tilde{\mu}_H);(\boldsymbol{\psi}_H,\mu_H);(\tilde{\boldsymbol{e}},\tilde{\varepsilon},\tilde{e}^{\theta})) = \\ &\qquad - L((\boldsymbol{u}_H,p_H,\theta_H);(\tilde{\boldsymbol{e}},\tilde{\varepsilon},\tilde{e}^{\theta})) - \mathcal{R}^{\mathrm{pr}}((\tilde{\boldsymbol{u}}_H,\tilde{p}_H,\tilde{\theta}_H);(\tilde{\boldsymbol{\psi}}_H,\tilde{\lambda}_H,\tilde{\mu}_H)) \\ &\qquad\qquad + F((\tilde{\boldsymbol{e}},\tilde{e}^{\theta}),(\tilde{\boldsymbol{e}},\tilde{e}^{\theta}),(\tilde{\boldsymbol{\psi}}_H,\tilde{\mu}_H))) \\ &\quad + \Big[E_1((\tilde{\boldsymbol{u}}_H,\tilde{\theta}_H);(\tilde{\boldsymbol{\psi}}_H,\tilde{\mu}_H),(\tilde{\boldsymbol{e}},\tilde{\varepsilon})) - E_1((\boldsymbol{u}_H,\theta_H);(\boldsymbol{\psi}_H,\mu_H),(\tilde{\boldsymbol{e}},\tilde{\varepsilon}))\Big] \\ &\qquad + \Big[L((\tilde{\boldsymbol{u}}_H,\tilde{p}_H,\tilde{\theta}_H);(\tilde{\boldsymbol{e}},\tilde{\varepsilon},\tilde{e}^{\theta})) - L((\boldsymbol{u}_H,p_H,\theta_H);(\tilde{\boldsymbol{e}},\tilde{\varepsilon},\tilde{e}^{\theta}))\Big]. \end{aligned} \tag{40}$$

Now, combining Eqs. (37), (38), (39), and (40), we write

$$
\begin{aligned}
0 = &\mp 2\kappa^u E_0((\hat{\boldsymbol{e}}^{\pm}, \hat{\varepsilon}^{\pm}, 0)), (\tilde{\boldsymbol{e}}, \tilde{\varepsilon}, 0)) \mp 2\kappa^u E_0(\boldsymbol{0}, 0, \hat{e}^{\theta,\pm})), (\boldsymbol{0}, 0, \tilde{e}^{\theta})) \\
&\pm \kappa^u E_0((\tilde{\boldsymbol{e}}, \tilde{\varepsilon}, \tilde{e}^{\theta}), (\tilde{\boldsymbol{e}}, \tilde{\varepsilon}, 0)) \pm \kappa^u E_1((\tilde{\boldsymbol{u}}_H, \tilde{\theta}_H); (\tilde{\boldsymbol{e}}, \tilde{e}^{\theta}), (\tilde{\boldsymbol{e}}, 0)) \\
&\pm \kappa^{\theta} E_0((\tilde{\boldsymbol{e}}, \tilde{\varepsilon}, \tilde{e}^{\theta}), (\boldsymbol{0}, 0, \tilde{e}^{\theta})) \pm \kappa^{\theta} E_1((\tilde{\boldsymbol{u}}_H, \tilde{\theta}_H); (\tilde{\boldsymbol{e}}, \tilde{e}^{\theta}), (\boldsymbol{0}, 0, \tilde{e}^{\theta})) \\
&\pm \kappa^u F((\tilde{\boldsymbol{e}}, \tilde{e}^{\theta}), (\tilde{\boldsymbol{e}}, \tilde{e}^{\theta}), (\tilde{\boldsymbol{e}}, 0)) \pm \kappa^{\theta} F((\tilde{\boldsymbol{e}}, \tilde{e}^{\theta}), (\tilde{\boldsymbol{e}}, \tilde{e}^{\theta}), (\boldsymbol{0}, \tilde{e}^{\theta})) \\
&+ L((\boldsymbol{u}_H, p_H, \theta_H); (\tilde{\boldsymbol{e}}, \tilde{\varepsilon}, \tilde{e}^{\theta})) + \mathcal{R}^{\mathrm{pr}}(\tilde{\boldsymbol{u}}_H, \tilde{p}_H, \tilde{\theta}_H); (\tilde{\boldsymbol{\psi}}_H, \tilde{\lambda}_H, \tilde{\mu}_H)) \\
&- F((\tilde{\boldsymbol{e}}, \tilde{e}^{\theta}), (\tilde{\boldsymbol{e}}, \tilde{e}^{\theta}), (\tilde{\boldsymbol{\psi}}_H, \tilde{\mu}_H)) \\
&- \Big[E_1((\tilde{\boldsymbol{u}}_H, \tilde{\theta}_H); (\tilde{\boldsymbol{\psi}}_H, \tilde{\mu}_H), (\tilde{\boldsymbol{e}}, \tilde{e}^{\theta})) - E_1((\boldsymbol{u}_H, \theta_H); (\boldsymbol{\psi}_H, \mu_H), (\tilde{\boldsymbol{e}}, \tilde{e}^{\theta})) \Big] \\
&- \Big[L((\tilde{\boldsymbol{u}}_H, \tilde{p}_H, \tilde{\theta}_H); (\tilde{\boldsymbol{e}}, \tilde{\varepsilon}, \tilde{e}^{\theta})) - L((\boldsymbol{u}_H, p_H, \theta_H); (\tilde{\boldsymbol{e}}, \tilde{\varepsilon}, \tilde{e}^{\theta})) \Big]. \qquad (41)
\end{aligned}
$$

If we insert Eq. (41) into the bound equation, Eq. (25), noting that

$$
\begin{aligned}
E_0((\tilde{\boldsymbol{e}}, \tilde{\varepsilon}, \tilde{e}^{\theta}), (\tilde{\boldsymbol{e}}, \tilde{\varepsilon}, 0)) &= E_0((\tilde{\boldsymbol{e}}, \tilde{\varepsilon}, 0), (\tilde{\boldsymbol{e}}, \tilde{\varepsilon}, 0)) \\
E_0((\tilde{\boldsymbol{e}}, \tilde{\varepsilon}, \tilde{e}^{\theta}), (\boldsymbol{0}, 0, \tilde{e}^{\theta})) &= E_0((\boldsymbol{0}, 0, \tilde{e}^{\theta}), (\boldsymbol{0}, 0, \tilde{e}^{\theta})),
\end{aligned}
$$

we find the following bound error expression

$$
s_H^{\pm} = s_h \pm D^{\pm} + I^{\pm},
$$

where

$$
D^{\pm} = \kappa^u \mathcal{F}_0(\tilde{\boldsymbol{e}} - \hat{\boldsymbol{e}}^{\pm}, \tilde{\varepsilon} - \hat{\varepsilon}^{\pm}, 0) + \kappa^{\theta} \mathcal{F}_0(\boldsymbol{0}, 0, \tilde{e}^{\theta} - \hat{e}^{\theta}),
$$

and $I^{\pm} = \sum_{j=1}^{6} I_j^{\pm}$. In these expressions, $\mathcal{F}_0(\boldsymbol{v}, q, \phi) = E_0((\boldsymbol{v}, q, \phi), (\boldsymbol{v}, q, \phi))$, and

$$
\begin{aligned}
I_1^{\pm} =& - F((\tilde{\boldsymbol{e}}, \tilde{e}^{\theta}), (\tilde{\boldsymbol{e}}, \tilde{e}^{\theta}), (\tilde{\boldsymbol{\psi}}_H, \tilde{\mu}_H))), \\
I_2^{\pm} =& \pm \kappa^u E_1((\tilde{\boldsymbol{u}}_H, \tilde{\theta}_H); (\tilde{\boldsymbol{e}}, \tilde{e}^{\theta}), (\tilde{\boldsymbol{e}}, 0)) \\
&\pm \kappa^{\theta} E_1((\tilde{\boldsymbol{u}}_H, \tilde{\theta}_H); (\tilde{\boldsymbol{e}}, \tilde{e}^{\theta}), (\boldsymbol{0}, \tilde{e}^{\theta})), \\
I_3^{\pm} =& \pm \kappa^u F((\tilde{\boldsymbol{e}}, \tilde{e}^{\theta}), (\tilde{\boldsymbol{e}}, \tilde{e}^{\theta}), (\tilde{\boldsymbol{e}}, 0)) \pm \kappa^{\theta} F((\tilde{\boldsymbol{e}}, \tilde{e}^{\theta}), (\tilde{\boldsymbol{e}}, \tilde{e}^{\theta}), (\boldsymbol{0}, \tilde{e}^{\theta})), \\
I_4^{\pm} =& - M(\tilde{\boldsymbol{e}}, \tilde{\boldsymbol{e}}), \\
I_5^{\pm} =& E_1((\boldsymbol{u}_H, \theta_H); (\boldsymbol{\psi}_H, \mu_H), (\tilde{\boldsymbol{e}}, \tilde{e}^{\theta})) - E_1((\tilde{\boldsymbol{u}}_H, \tilde{\theta}_H); (\tilde{\boldsymbol{\psi}}_H, \tilde{\mu}_H), (\tilde{\boldsymbol{e}}, \tilde{e}^{\theta})), \\
I_6^{\pm} =& L((\boldsymbol{u}_H, p_H, \theta_H); (\tilde{\boldsymbol{e}}, \tilde{\varepsilon}, \tilde{e}^{\theta})) - L((\tilde{\boldsymbol{u}}_H, \tilde{p}_H, \tilde{\theta}_H); (\tilde{\boldsymbol{e}}, \tilde{\varepsilon}, \tilde{e}^{\theta})).
\end{aligned}
$$

4 Convergence of the Indefinite Terms

We give here explicit expressions for the indefinite terms, $I_{1,\cdots,6}$, defined in Appendix 3,

$$
\begin{aligned}
|I_1^{\pm}| &= |\int_\Omega \tilde{e}_i \tilde{e}_j \frac{\partial \tilde{\psi}_{H,i}}{\partial x_j}\, d\Omega + \int_\Omega \tilde{e}^\theta \tilde{e}_j \frac{\partial \tilde{\mu}_H}{\partial x_j}\, d\Omega|, \\
|I_2^{\pm}| &= |\kappa^u \left[\int_\Omega \tilde{u}_{H,i} \tilde{e}_j \frac{\partial \tilde{e}_i}{\partial x_j}\, d\Omega + \int_\Omega \tilde{e}_i \tilde{u}_{H,j} \frac{\partial \tilde{e}_i}{\partial x_j}\, d\Omega \right] \\
&\quad + \kappa^\theta \left[\int_\Omega \tilde{\theta}_H \tilde{e}_j \frac{\partial \tilde{e}^\theta}{\partial x_j}\, d\Omega + \int_\Omega \tilde{e}^\theta \tilde{u}_{H,j} \frac{\partial \tilde{e}^\theta}{\partial x_j}\, d\Omega \right] \\
&\quad + \beta \int_\Omega \hat{g}_i \tilde{e}_i \tilde{e}^\theta\, d\Omega|, \\
|I_3^{\pm}| &= |\kappa^u \int_\Omega \tilde{e}_i \tilde{e}_j \frac{\partial \tilde{e}_i}{\partial x_j}\, d\Omega + \kappa^\theta \int_\Omega \tilde{e}^\theta \tilde{e}_j \frac{\partial \tilde{e}^\theta}{\partial x_j}\, d\Omega|, \\
|I_4^{\pm}| &= |m(\tilde{\boldsymbol{e}}, \tilde{\boldsymbol{e}})|, \\
|I_5^{\pm}| &= |\int_\Omega u_{H,i} \psi_{H,j} \frac{\partial \tilde{e}_i}{\partial x_j}\, d\Omega + \int_\Omega \psi_{H,i} u_{H,j} \frac{\partial \tilde{e}_i}{\partial x_j}\, d\Omega + \int_\Omega \theta_H \psi_{H,j} \frac{\partial \tilde{e}^\theta}{\partial x_j}\, d\Omega \\
&\quad + \int_\Omega \mu_H u_{H,j} \frac{\partial \tilde{e}^\theta}{\partial x_j}\, d\Omega - \int_\Omega \tilde{u}_{H,i} \tilde{\psi}_{H,j} \frac{\partial \tilde{e}_i}{\partial x_j}\, d\Omega - \int_\Omega \tilde{\psi}_{H,i} \tilde{u}_{H,j} \frac{\partial \tilde{e}_i}{\partial x_j}\, d\Omega \\
&\quad - \int_\Omega \tilde{\theta}_H \tilde{\psi}_{H,j} \frac{\partial \tilde{e}^\theta}{\partial x_j}\, d\Omega - \int_\Omega \tilde{\mu}_H \tilde{u}_{H,j} \frac{\partial \tilde{e}^\theta}{\partial x_j}\, d\Omega|, \\
|I_6^{\pm}| &= 2|m(\boldsymbol{u}_H - \tilde{\boldsymbol{u}}_H, \tilde{\boldsymbol{e}})|.
\end{aligned}
$$

We also note that

$$
\begin{aligned}
|\tilde{\boldsymbol{e}}|_{H^1(\Omega)} &= |\boldsymbol{u}_h - \tilde{\boldsymbol{u}}_H|_{H^1(\Omega)} \\
&\leq |\boldsymbol{u}_h - \boldsymbol{u}_H|_{H^1(\Omega)} + |\boldsymbol{u}_H - \tilde{\boldsymbol{u}}_H|_{H^1(\Omega)} \\
&\leq C|\boldsymbol{u}_h - \boldsymbol{u}_H|_{H^1(\Omega)} \leq CH^2,
\end{aligned}
$$

assuming that $\boldsymbol{u} \in H^3(\Omega) \times H^3(\Omega)$. Similarly, we have

$$||\tilde{\boldsymbol{e}}||_{L^2(\Omega)} \leq ||\boldsymbol{u}_h - \boldsymbol{u}_H||_{L^2(\Omega)} + CH|\boldsymbol{u}_h - \boldsymbol{u}_H|_{H^1(\Omega)} \leq CH^3.$$

This result is directly useful to prove, for instance, that, in term $I_6^{\pm}$,

$$m(\boldsymbol{u}_H - \tilde{\boldsymbol{u}}_H, \tilde{\boldsymbol{e}}) \leq C||\boldsymbol{u}_H - \tilde{\boldsymbol{u}}_H||_{L^2(\Omega)} ||\tilde{\boldsymbol{e}}||_{L^2(\Omega)} \leq CH^6,$$

where we have used the above estimates.

We will now estimate the convergence rates of two (representative) selected terms in $\sum_{i=1}^{6}|I_i^{\pm}|$. The convergence rates of the other terms are obtained by similar arguments.

We first consider a term in $|I_1^{\pm}|$,

$$
\begin{aligned}
|\int_\Omega \tilde{e}_i\tilde{e}_j \frac{\partial \tilde{\psi}_{H,i}}{\partial x_j}\, d\Omega| &\le |\int_\Omega \tilde{e}_i\tilde{e}_j \frac{\partial \tilde{\psi}_{H,i}-\psi_i}{\partial x_j}\, d\Omega| + |\int_\Omega \tilde{e}_i\tilde{e}_j \frac{\partial \psi_i}{\partial x_j}\, d\Omega|, \\
&\le ||\tilde{\boldsymbol{e}}||_{L^4(\Omega)}||\tilde{\boldsymbol{e}}||_{L^4(\Omega)}||\nabla(\tilde{\boldsymbol{\psi}}_H-\boldsymbol{\psi})||_{L^2(\Omega)} \\
&\quad + ||\tilde{\boldsymbol{e}}||_{L^2(\Omega)}||\tilde{\boldsymbol{e}}||_{L^4(\Omega)}||\nabla\boldsymbol{\psi}||_{L^4(\Omega)},
\end{aligned}
$$

where we have used the Cauchy-Schwartz inequality. By virtue of the Sobolev inequality, $||v||_{L^4(\Omega)} \le C||v||_{H^1(\Omega)}$, $\forall v \in H^1(\Omega)$ (see, *e.g.*, [1]), we now write

$$
\begin{aligned}
|\int_\Omega \tilde{e}_i\tilde{e}_j \frac{\partial \tilde{\psi}_{H,i}}{\partial x_j}\, d\Omega| &\le C_1||\tilde{\boldsymbol{e}}||_{H^1(\Omega)}||\tilde{\boldsymbol{e}}||_{H^1(\Omega)}|\tilde{\boldsymbol{\psi}}_H-\boldsymbol{\psi}|_{H^1(\Omega)} \\
&\quad + C_2||\tilde{\boldsymbol{e}}||_{L^2(\Omega)}||\tilde{\boldsymbol{e}}||_{H^1(\Omega)}||\boldsymbol{\psi}||_{H^2(\Omega)} \\
&\le C_1H^6 + C_2H^5,
\end{aligned}
$$

where we have exploited our previous estimates; here C_1 and C_2 denote two generic positive constants independent of H, and we have assumed $\boldsymbol{u}, \boldsymbol{\psi} \in H^3(\Omega)\times H^3(\Omega)$.

For our second example, we rewrite $|I_5^{\pm}|$ as

$$
\begin{aligned}
|I_5^{\pm}| = |\int_\Omega (u_{H,i}-\tilde{u}_{H,i})\psi_{H,j}\frac{\partial \tilde{e}_i}{\partial x_j}\, d\Omega &+ \int_\Omega \tilde{u}_{H,i}(\psi_{H,j}-\tilde{\psi}_{H,j})\frac{\partial \tilde{e}_i}{\partial x_j}\, d\Omega \\
+ \int_\Omega \psi_{H,i}(u_{H,j}-\tilde{u}_{H,j})\frac{\partial \tilde{e}_i}{\partial x_j}\, d\Omega &+ \int_\Omega (\psi_{H,i}-\tilde{\psi}_{H,i})\tilde{u}_{H,j}\frac{\partial \tilde{e}_i}{\partial x_j}\, d\Omega \\
+ \int_\Omega \theta_H(\psi_{H,j}-\tilde{\psi}_{H,j})\frac{\partial \tilde{e}^\theta}{\partial x_j}\, d\Omega &+ \int_\Omega \mu_H(u_{H,j}-\tilde{u}_{H,j})\frac{\partial \tilde{e}^\theta}{\partial x_j}\, d\Omega|,
\end{aligned}
$$

and we consider, for instance,

$$
\begin{aligned}
|\int_\Omega (u_{H,i}-\tilde{u}_{H,i})\psi_{H,j}\frac{\partial \tilde{e}_i}{\partial x_j}\, d\Omega| &\le |\int_\Omega (u_{H,i}-\tilde{u}_{H,i})(\psi_{H,j}-\psi_j)\frac{\partial \tilde{e}_i}{\partial x_j}\, d\Omega| \\
&\quad + |\int_\Omega (u_{H,i}-\tilde{u}_{H,i})\psi_j\frac{\partial \tilde{e}_i}{\partial x_j}\, d\Omega| \\
&\le C_1||\boldsymbol{u}_H-\tilde{\boldsymbol{u}}_H||_{L^4(\Omega)}||\boldsymbol{\psi}_H-\boldsymbol{\psi}||_{L^4(\Omega)}|\tilde{\boldsymbol{e}}|_{H^1(\Omega)} \\
&\quad + C_2||\boldsymbol{u}_H-\tilde{\boldsymbol{u}}_H||_{L^2(\Omega)}||\boldsymbol{\psi}||_{L^\infty(\Omega)}|\tilde{\boldsymbol{e}}|_{H^1(\Omega)}.
\end{aligned}
$$

If we recall the inequality $||\boldsymbol{\psi}||_{L^\infty(\Omega)} \leq C||\boldsymbol{\psi}||_{H^2(\Omega)}$ (see, *e.g.*, [1]), and if we use our previous estimates, then we find

$$
\begin{aligned}
|\int_\Omega (u_{H,i} - \tilde{u}_{H,i})\psi_{H,j}\frac{\partial \tilde{e}_i}{\partial x_j}\, d\Omega| \leq\ & C_1||\boldsymbol{u}_H - \tilde{\boldsymbol{u}}_H||_{H^1(\Omega)}||\boldsymbol{\psi}_H - \boldsymbol{\psi}||_{H^1(\Omega)}|\tilde{\boldsymbol{e}}|_{H^1(\Omega)} \\
& + C_2||\boldsymbol{u}_H - \tilde{\boldsymbol{u}}_H||_{L^2(\Omega)}||\boldsymbol{\psi}||_{H^2(\Omega)}|\tilde{\boldsymbol{e}}|_{H^1(\Omega)} \\
\leq\ & C_1 H^6 + C_2 H^5.
\end{aligned}
$$

Acknowledgments

This work was supported by NASA Grants NAG1-1978, NAG1-1587, and NAG4-105, DARPA and ONR Grant N00014-91-J-1-1889, and AFOSR Grant F49620-97-1-0052. L.M. was partially supported by Fulbright, BAEF, and NATO Fellowships. We would like to acknowledge our longstanding and very fruitful collaboration with Prof. Y. Maday of Université Pierre et Marie Curie, Paris, France.

References

[1] R. A. Adams. *Sobolev Spaces.* Academic Press, New York, 1975.

[2] M. Ainsworth and J. T. Oden. A posteriori error estimation in finite element analysis. *Comp. Meth. in Appl. Mech. and Engrg.*, 142:1–88, 1997.

[3] R. E. Bank and A. Weiser. Some a posteriori error estimators for elliptic partial differential equations. *Math. Comp.*, 44(170):283–301, 1985.

[4] R. Becker and R. Rannacher. A feedback approach to error control in finite element method: Basic analysis and examples. *East-West J. Numer. Math.*, 4:237–264, 1996.

[5] M. Crouzeix and P.-A. Raviart. Conforming and non-conforming finite element methods for solving the stationary Stokes equation. *RAIRO Anal. Numer.*, 7:33–76, 1973.

[6] C. Farhat and J. Mandel. Scalable substructuring by Lagrange multipliers in theory and practice. In P. Bjorstad, M. Espedal, and D. Keyes, editors, *Domain Decomposition Methods for Partial Differential Equations.* Wiley and Sons, 1998. In press.

[7] P. Ladeveze and D. Leguillon. Error estimation procedures in the finite element method and applications. *SIAM J. Numer. Anal.*, 20:485–509, 1983.

[8] L. Machiels, A. T. Patera, J. Peraire, and Y. Maday. A general framework for finite element a posteriori error control: application to linear and nonlinear convection-dominated problems. Proceedings of ICFD Conference, Oxford, 1998.

[9] L. Machiels, J. Peraire, and A. T. Patera. Output bound approximations for partial differential equations; application to the incompressible Navier–Stokes equations. In S. Biringen, editor, *Proceedings of the Istanbul Workshop on Industrial and Environmental Applications of Direct and Large Eddy Numerical Simulation*. Springer-Verlag, August 1998.

[10] Y. Maday and A. T. Patera. Numerical analysis of a posteriori finite element bounds for linear-functional outputs. Mathematical Models and Methods in Applied Science, to appear.

[11] Y. Maday, A. T. Patera, and J. Peraire. A general formulation for a posteriori bounds for output functionals of partial differential equations; application to the eigenvalue problem. C.R. Acad. Sci. Paris, to appear.

[12] J. Mandel and M. Brezina. Balancing domain decomposition: theory and performance in two and three dimensions. Technical report, Center for Computational Mathematics, University of Colorado at Denver, Denver, CO 80217-3364, 1993.

[13] M. Paraschivoiu and A. T. Patera. A posteriori bounds for linear-functional outputs of Crouzeix-Raviart finite element discretizations of the incompressible Stokes problem. Int. J. for Num. in Fluids, to appear.

[14] M. Paraschivoiu and A. T. Patera. A hierarchical duality approach to bounds for the outputs of partial differential equation. *Comp. Meth. in Appl. Mech. and Engrg.*, 158:389–407, 1998.

[15] M. Paraschivoiu, J. Peraire, and A. T. Patera. A posteriori finite element bounds for linear-functional outputs of elliptic partial differential equations. *Comp. Meth. in Appl. Mech. and Engrg.*, 150:289–312, 1997.

[16] A. T. Patera and E. M. Ronquist. A general output bound result: application to discretization and iteration error estimation and control. Mathematical Models and Methods in Applied Science, submitted.

[17] J. Peraire and A. T. Patera. Bounds for linear-functional outputs of coercive partial differential equations: local indictors and adaptive refinement. In P. Ladeveze and J. T. Oden, editors, *On New Advances in Adaptive Computational Methods in Mechanics*, 1997.